

## ATLANTIC FOR THE LAST 225,000 YEARS

*Laura F. Robinson, Jess F. Adkins, Daniel S. Scheirer,  
Diego P. Fernandez, Alexander Gagnon, and Rhian G. Waller*

## ABSTRACT

Deep-sea corals have grown for over 200,000 yrs on the New England Seamounts in the northwest Atlantic, and this paper describes their distribution both with respect to depth and time. Many thousands of fossil scleractinian corals were collected on a series of cruises from 2003–2005; by contrast, live ones were scarce. On these seamounts, the depth distribution of fossil *Desmophyllum dianthus* (Esper, 1794) is markedly different to that of the colonial scleractinian corals, extending 750 m deeper in the water column to a distinct cut-off at 2500 m. This cut-off is likely to be controlled by the maximum depth of a notch-shaped feature in the seamount morphology. The ages of *D. dianthus* corals as determined by U-series measurements range from modern to older than 200,000 yrs. The age distribution is not constant over time, and most corals have ages from the last glacial period. Within the glacial period, increases in coral population density at Muir and Manning Seamounts coincided with times at which large-scale ocean circulation changes have been documented in the deep North Atlantic. Ocean circulation changes have an effect on coral distributions, but the cause of the link is not known.

The deep ocean has an important role in modulating global climate: its circulation transports heat across the equator and it acts as the major sink for carbon dioxide. During the last million years two dramatic types of climate change are obvious in geologic records, 100,000 yr glacial-interglacial oscillations (Imbrie et al., 1984) and abrupt millennial scale climate changes during the last glacial period (Grootes et al., 1993). The mechanisms driving these climate oscillations have not yet been fully explained, but it is likely that ocean circulation is critical to both (Broecker, 1998).

Geochemical reconstructions have demonstrated that circulation in the glacial Atlantic was different than today (Duplessy et al., 1988; Oppo and Lehman, 1993; Curry and Oppo, 2005). At the latitude of the New England Seamounts, northern-source deep water shoaled to ~2000 m water depth and was replaced by southern-source water. During the deglaciation the climate switched between warm and cool conditions (Grootes et al., 1993). At the same time the North Atlantic circulation pattern switched between glacial-like and modern-like circulation pattern (Boyle and Keigwin, 1987; Marchitto et al., 1998). At intermediate depths (< 2500 m) ocean circulation was also variable, with large changes in water-mass properties occurring on decadal timescales, but these changes were not always associated with the most obvious climate events (Robinson et al., 2005).

One of the most striking records of climate changes in North Atlantic marine sediments is the presence of Heinrich events, characterized by anomalous occurrences of ice-rafted debris (Heinrich, 1988). The large volumes of fresh water associated with melting ice may have decreased the rate of North Atlantic Deep Water (NADW) formation, together with a slow down in the overall ventilation rate of the oceans (Rahmstorf, 1995). Strong evidence in the form of ( $^{231}\text{Pa}/^{230}\text{Th}$ ) ratios recorded in

deep-sea sediments support just such a reduction in the circulation rate of NADW at Heinrich event 1 and the Younger Dryas (McManus et al., 2004).

Since about half of the deep-water formation in the modern ocean occurs in the North Atlantic (Broecker et al., 1998; Ganachaud and Wunsch, 2000), the northwest Atlantic basin is a location of particular interest for investigating the links between ocean circulation and climate. However, constructing high-resolution deep-sea records can be challenging because sedimentary cores tend to be mixed by bioturbation, smoothing the signals of rapid change in the deep ocean. One way to alleviate this difficulty is to analyze the chemical composition of deep-sea coral skeletons.

Deep-sea corals have been found at depths ranging from 0 to 5000 m in all of the major ocean basins (Freiwald, 2002). The chemical composition of the aragonite skeletons of scleractinian corals is affected by: (a) the composition of the seawater in which they grow, (b) environmental parameters, such as temperature, and (c) biological vital effects (Shen and Boyle, 1988; Smith et al., 1997; Adkins et al., 1998, 2003; Mangini et al., 1998; Cohen et al., 2001; Goldstein et al., 2001; Meibom et al., 2003; Schroder-Ritzrau et al., 2003; Frank et al., 2004; Bond et al., 2005; Robinson et al., 2005). Since corals live for long time periods, and their skeletons are preserved when they die, they form a unique archive of ocean conditions in the past. Indeed, multiple sub-samples taken carefully from one specimen can be used to generate a time series of changes that occurred in the ocean during the lifetime of the coral (Adkins et al., 1998). The high uranium content of aragonite (~3 ppm) makes some species of deep-sea coral well suited to precise U-Th analyses allowing absolute ages to be measured over many hundreds of thousands of years. Such dating allows us to link records from multiple fossil individuals to look at even longer time periods (Robinson et al., 2005).

The New England Seamounts are well located to capture variability in deep Atlantic circulation (Fig. 1). Both fossil and modern deep-sea corals were collected from these seamounts more than 45 yrs ago on RV ATLANTIS cruises 260 and 280. More recently over 3500 solitary and 10s of kilograms of colonial scleractinian corals (Fig. 2) were collected from the New England Seamounts in May/June 2003 (Adkins and Scheirer, 2003). Use of the deep submergence vehicle DSV ALVIN ensured that the depth of each coral was well known, and the corals were collected at, or near to, life position. Additional samples were collected during a second DSV ALVIN cruise and an remotely operated vehicle ROV HERCULES cruise in 2005, covering both the New England Seamounts and the Corner Rise Seamounts. Here we describe the distribution of deep-sea corals both with depth and time in the North Atlantic, and how they may be linked to changes in deep-water circulation. Understanding these changes is important when using corals for paleo-climate reconstructions, and also for understanding the modern day distribution of deep-sea coral populations.

## METHODS

All samples were collected using deep submergence vehicles (DSV ALVIN or the ROV HERCULES) and a netted basket was used to "scoop" up corals from on the sea floor. Corals were counted, weighed, and archived at Caltech. A random selection of coral individuals from each depth and seamount was taken for U-series analysis. A potential bias in the final age distribution is that each coral selected must contain sufficient carbonate (i.e., biased towards larger individuals). A 0.5–1.0 g piece of carbonate was taken from each of 127 corals, with a total of 159 U-Th analyses. Visible ferromanganese crust was physically removed from each sample,

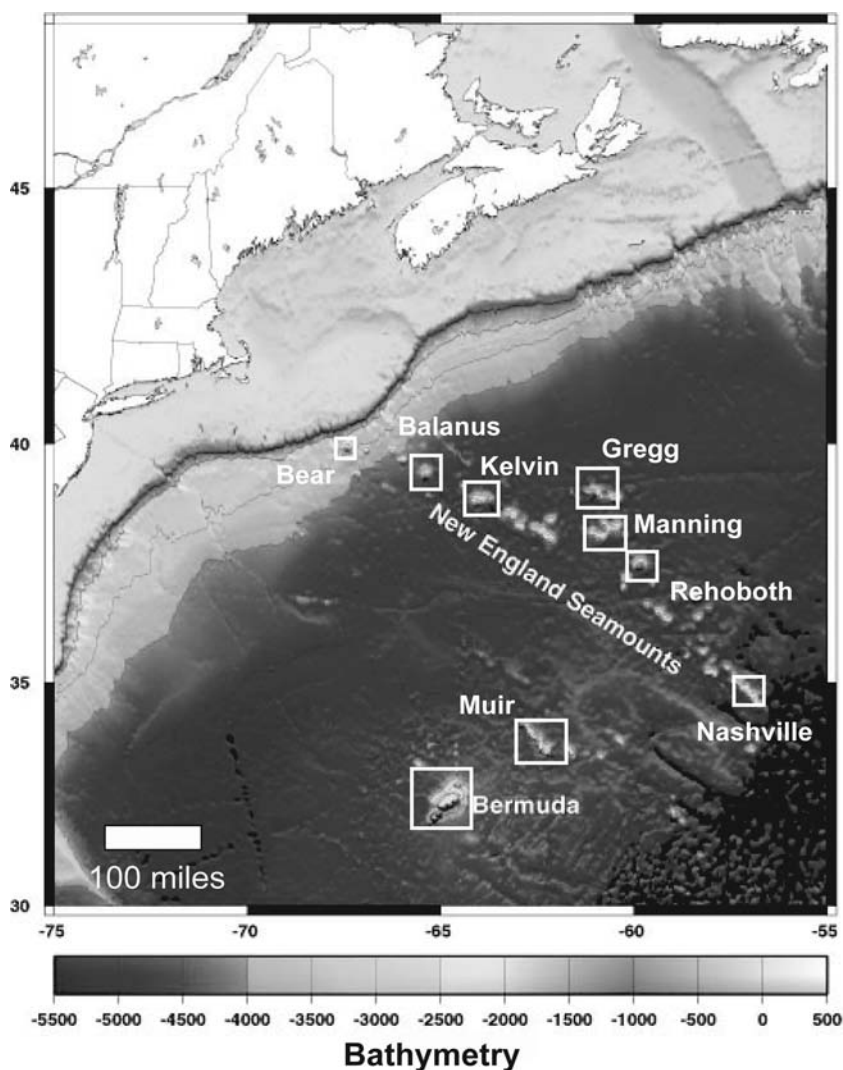


Figure 1. Map of New England Seamounts showing location of seamounts from which deep-sea corals were collected during three cruises from 2003–2006.

and holes formed by endolithic organisms were drilled out using a dremel tool. Each sample was subjected to a rigorous chemical cleaning procedure designed to remove the remaining ferromanganese crust (Cheng et al., 2000). Dissolved samples were spiked with a mixed  $^{229}\text{Th}$ – $^{236}\text{U}$  spike, and U and Th were separated and purified by anion-exchange chemistry (Edwards et al., 1986). The spike ratio was calibrated to a 2 SD uncertainty of 0.4% using HU-1, a U-series standard close to secular equilibrium (Cheng et al., 2000). Purified aliquots of U and Th were measured by Neptune multi-collector inductively coupled mass spectrometer (MC-ICP-MS) with bracketing standards of CRM-145 for U, and an in-house Th standard calibrated against CRM-145 (Robinson et al., 2002, 2005). Procedural blanks had an average value of 67 pg for  $^{238}\text{U}$  (< 0.002% of the typical sample size) and 2 fg for  $^{230}\text{Th}$ . The  $^{232}\text{Th}$  concentration in each sample was measured to quantify remaining contamination from Th-rich ferromanganese crust. This  $^{232}\text{Th}$ -based estimate was used to correct for initial  $^{230}\text{Th}$  using a  $^{232}\text{Th}/^{230}\text{Th}$  ratio of  $12,500 \pm 12,500$  (Cheng et al., 2000).

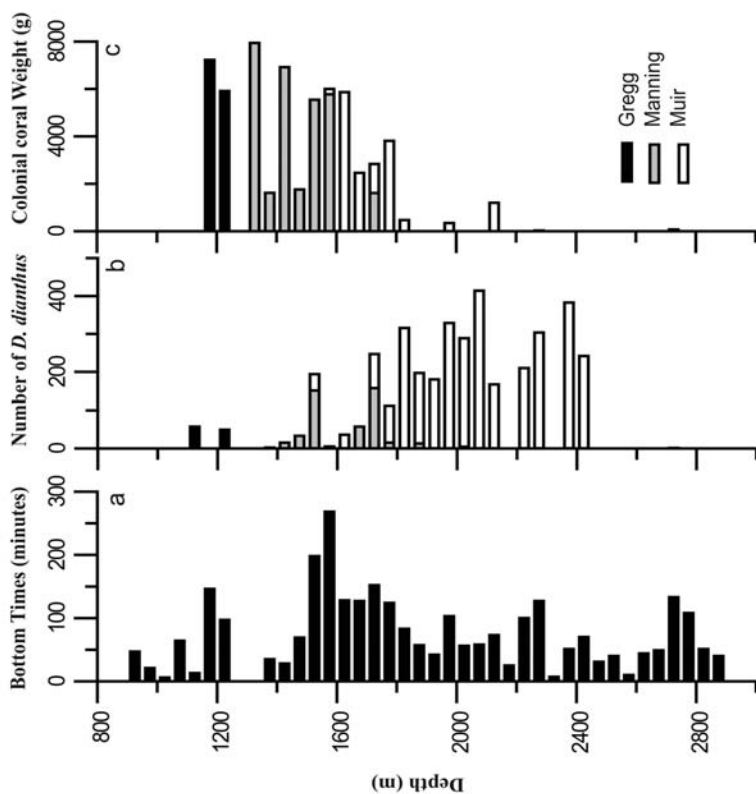


Figure 2. Depth distribution of the samples collected during the DSV ALVIN cruise to the New England Seamounts in 2003. (A) Time in minutes spent at the bottom; (B) number of *Desmophyllum dianthus* collected; and (C) weight of colonial corals collected, including *Enallopsammia*, *Lophelia*, and *Solenosmilia*. Although significant time was spent at depths > 2500 m, very few corals were recovered. Black bars are from Gregg Seamount, grey bars are from Manning Seamount, and white bars are from Muir Seamount.

## RESULTS

Most of the samples discussed herein were collected in May/June 2003 on DSV ALVIN cruise AT7\_35 to Manning, Muir, and Gregg Seamounts (Adkins and Scheirer, 2003) (Fig. 1). During 3190 min (53 hrs, 10 min) of DSV ALVIN bottom time ranging in depth from 920 to 2870 m, we collected more than 3700 individual fossil *Desmophyllum dianthus* (Esper, 1794) and more than 60 kg of colonial corals (Fig. 2). The deepest colonial fossil coral sample was collected from ~2750 m, but > 95% of samples ranged from 1175–1800 m. By contrast 99% of *D. dianthus* individuals were collected between 1175 m and 2550 m, with one deep sample collected at 2740 m (Fig. 2). At this location, the depth range of *D. dianthus*, reaches ~ 750 m deeper than the colonial scleractinians. In June 2003 further DSV ALVIN sampling (Cruise AT8-1.) on an Ocean Exploration cruise “Mountains in the Sea” recovered further fossil corals, including samples from Kelvin and Bear Seamounts (Fig. 1). The ROV HERCULES cruise in August 2005 recovered more than 1300 fossil *D. dianthus* corals from the New England Seamounts and the Corner Rise Seamounts. The fossil depth

distribution from Muir, Manning, Nashville, Rehoboth, Kelvin, Balanus, and Gregg Seamounts are similar, considering the depth ranges to which dives were made. Only 15 modern *D. dianthus* individuals were collected from all of the New England Seamounts (Fig. 3). The range of modern *D. dianthus*; 1600–2200 m is similar to the fossil distribution, but the small number of modern samples collected precludes a statistical depth comparison between the two sample sets.

All U-series analyses data are recorded in Table 1, and some of these data have been presented previously (Robinson et al., 2005, 2006). A measure of the extent of diagenetic alteration to the U-series system is the ( $^{234}\text{U}/^{238}\text{U}$ ) ratio (where parentheses indicate activity ratio). Marine carbonates incorporate the isotopic ratio (denoted as  $\delta^{234}\text{U} = ([(^{234}\text{U}/^{238}\text{U})_{\text{meas}} / (^{234}\text{U}/^{238}\text{U})_{\text{eq}}] - 1) \times 10^3$ ) of the seawater in which they grow (Broecker and Takahashi, 1966; Robinson et al., 2004). This value is invariant throughout the water column (Cheng et al., 2000) and has been constant ( $\sim 146\%$ ) to within  $\sim 10\%$  over the last several hundred thousand years (Bard et al., 1991; Stirling et al., 1995; Henderson, 2002; Robinson et al., 2004). For a closed-system, the  $\delta^{234}\text{U}_{\text{initial}}$  ( $\delta^{234}\text{U}_{\text{initial}} = \delta^{234}\text{Ue}^{\lambda t}$ ) should be identical to that of the modern day (Edwards et al., 1986). Samples with  $\delta^{234}\text{U}_{\text{initial}}$  values different to modern seawater are likely to return inaccurate apparent ages (Gallup et al., 1994). Such changes may come about through processes such as open-system exchange with seawater or U-rich organic matter, or through internal re-arrangement of alpha-recoil mobilized  $^{234}\text{U}$  (e.g., Robinson et al., 2006). All of the data in the discussion focuses on samples with  $\delta^{234}\text{U}_{\text{initial}}$  values within 7‰ of modern seawater. Twenty-eight out of 127 corals lie outside the acceptable range (Table 2). Reliable ages range from 225–0.3 ka for *D. dianthus* (Fig. 4;  $n = 93$ ), 12.6–11.7 ka for *Caryophyllia* ( $n = 2$ ), 0.1–0.08 ka for *Solenosmilia* ( $n = 2$ ), and 0.2 ka for *Enallopsammia* ( $n = 1$ ). Ninety-six of these ages are from the Cruise AT7-35 (Adkins and Scheirer, 2003) and represent 2.7% of the sample collection from that cruise.

At one location we recovered a fallen gorgonian coral acting as a growth substrate for *D. dianthus*. Reliable ages for *D. dianthus* corals growing on the gorgonian range from 65 ka to 30 ka. Ages from the gorgonian itself were difficult to establish as the wide range of  $\delta^{234}\text{U}_{\text{initial}}$  values (151.4‰–187.8‰) indicate that its skeleton is more prone to diagenesis than scleractinians (Table 1). We have not yet carried out extensive studies to determine the potential for U-series dating in gorgonian corals.

## DISCUSSION

**DEPTH DISTRIBUTION.**—Attempts have been made to document the depth distributions of modern deep-sea corals (Freiwald, 2002), but the expense and logistical problems associated with exploring the deep-ocean floor has made a full inventory impossible. We know even less about the distributions of fossil deep-sea corals through depth or time. Our New England Seamount collection shows a distinct depth cut-off at 1800 m for colonial corals and 2500 m for *D. dianthus* in the fossil record. On Muir Seamount, most of the exploration was carried out in a deep notch between two peaks in the ridge. This notch provides a hard substrate and the seafloor experiences strong currents thought to be beneficial for coral growth. The maximum depth of the notch (2500 m) may be the cause of the paucity of scleractinian corals collected below 2500 m. A second notch farther east extends to much greater depths, and collections from this location would clarify whether the ridge morphology is

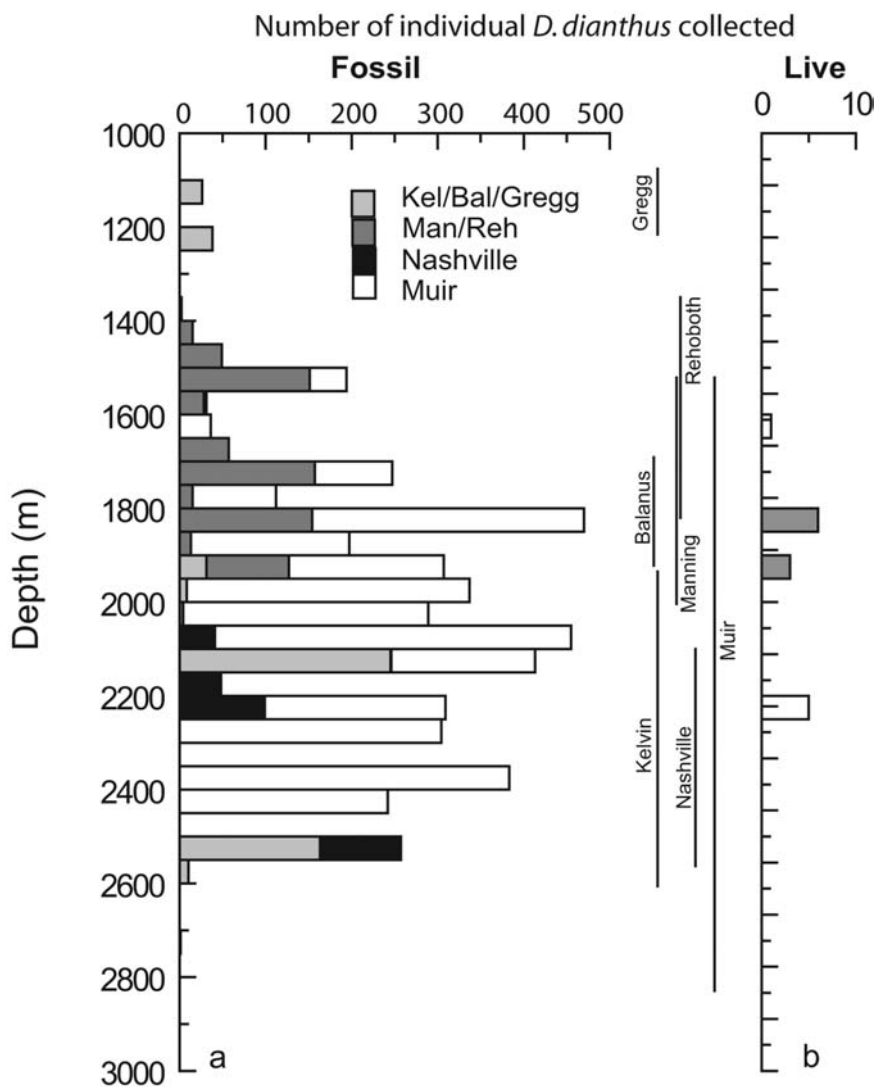


Figure 3. Depth distribution for fossil and live *Desmophyllum dianthus* collected during the DSV ALVIN cruise in 2003 and the ROV HERCULES cruise in 2005, highlighting the large number and depth range of fossil corals on all seamounts compared to live corals. The collection is only a subsample of the number of corals observed during these dives, especially with respect to fossil corals for which representative “scoops” of corals were taken from each sample site. The seamounts are grouped geographically, with Kelvin, Balanus, and Gregg the most northwesterly, Manning and Rehoboth in the middle of the chain, Nashville farther east, and Muir separate from the chain (see Fig. 1). Additional corals were collected from the Corner Rise Seamounts. The vertical lines demark the depths at which dives looking for corals took place. Few live specimens were recovered, despite focused searches to allow for modern studies.

indeed the major control on the depth distribution of *D. dianthus* collected on cruise AT7-35. This explanation, however, does not account for the depth distribution of the fossil colonial corals (*Solenosmilia*, *Lophelia*, and *Enallopsammia*) because they become less abundant at ~1800 m.

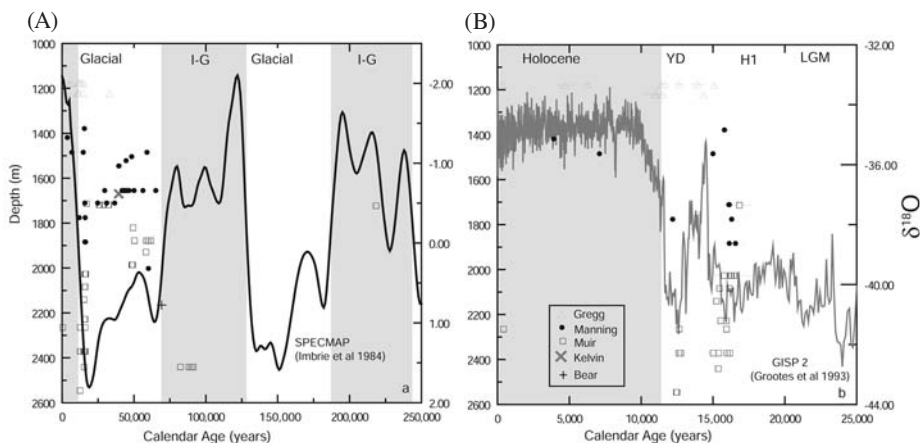


Figure 4. Ages and depths of dated fossil corals that have U-isotope ratios indicative of closed system behavior. (A) all of the dated *Desmophyllum dianthus* from Gregg, Manning, Bear, Kelvin, and Muir Seamounts. Ages range from 225 ka to modern. Additional age measurements from *Solenosmilia*, *Enallopsammia*, and *Caryophyllia* and from a gorgonian octocoral are shown in Table 1. The thick black line is the  $\delta^{18}\text{O}$  SPECMAP curve (Imbrie et al., 1984) where more negative values are indicative of interglacial conditions (shaded grey) and more positive values are indicative of glacial times. The majority of the coral ages lie within the last glacial period. (B) an enlargement of the last glacial maximum, the deglaciation, and the Holocene (shaded grey). The grey curve is the  $\delta^{18}\text{O}$  record from GISP 2 (Grootes et al., 1993). No corals have been found with ages within the Last Glacial Maximum (23–19 ka) as defined by the EPILOG working group (Mix et al., 2001).

A second factor that may impact the distribution of deep-sea corals is the properties of the water itself. The current velocity may affect either the range and distribution of coral larvae or the supply of food. Additionally, the properties of the water-mass bathing the seamount (e.g., nutrients, salinity or temperature) may be more or less beneficial to coral growth. The modern water column at the location of the New England Seamounts is filled by North Atlantic Deep Water (NADW), with no distinct depth gradients in nutrients, temperature, or salinity at the relevant depths. There is, therefore, no obvious water-mass property controlling the depth distribution of azooxanthellate scleractinians in the NW Atlantic today. However, at certain times in the past we know that the circulation pattern was different than the modern. For example, southern-sourced water was present up to depths of about 2000 m during the last glacial maximum (LGM) (Oppo and Lehman, 1993; Curry and Oppo, 2005). This water-mass boundary is close to the cut-off depth of *D. dianthus* and colonial scleractinians, suggestive of a link between ocean circulation and coral distribution. The best way to explore this relationship in detail is to examine the age distribution of the corals.

**AGE DISTRIBUTION.**—By looking at the ages of the New England Seamount *D. dianthus* populations we can learn more about the controls on their distribution, for example, whether the coral populations grew continuously over time, whether the population density was pulsed, and whether any such pulses are linked to known changes in the deep ocean. In the simplest case, the population has been stable. In the study area we found 15 live, and ~5000 fossil individuals. If we assume that each coral has a life span of ~100 yrs (Adkins et al., 2004) then a stable population could have persisted for ~35,000 yrs. We observe corals that are many times older than 35

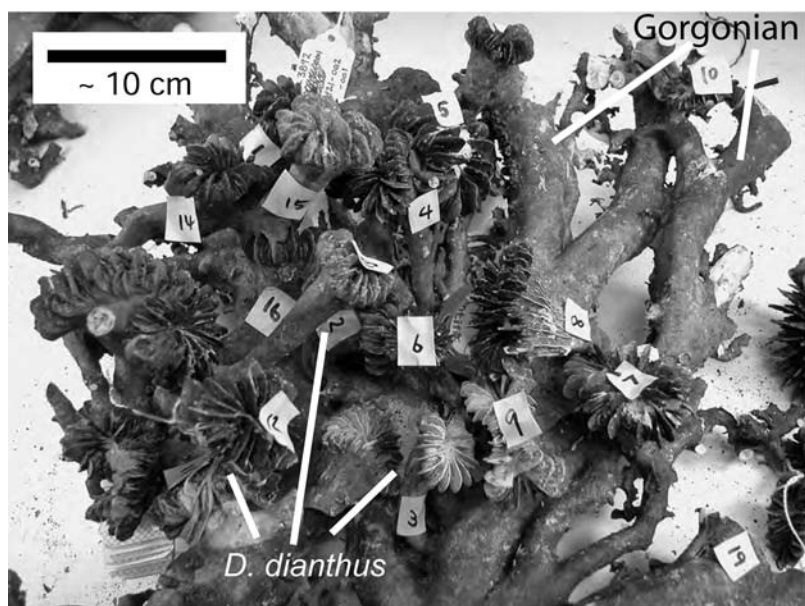


Figure 5. Portion of a deep-sea coral buildup. At the base, a large fallen gorgonian skeleton was oriented horizontally. Multiple *Desmophyllum dianthus* corals have grown both on the fallen gorgonian, and upon one another. Much of the structure is coated in a black or brown ferromanganese crust. This buildup acts as a natural, long-lived recruitment experiment allowing us to investigate the relative timing of deep-sea coral settling.

ka, our first indication that the population has not in fact been stable. The age distributions of corals from Muir and Manning Seamounts appear to be different to those from Gregg Seamount and are discussed separately below (Fig. 4a).

**MUIR AND MANNING SEAMOUNTS.**—Visually, it is clear that the growth of these corals is not randomly distributed through time, but that most of the corals grew during the last glacial period—i.e., from 70 to 10 ka (Fig. 4A). On Muir Seamount, farthest to the south, there are only five corals that grew during interglacials, and four of these were alive during Marine Isotope Stage (MIS) 5b. MIS 5b is a stadial near to the end of the last interglacial period when the deep-ocean temperature had already changed to glacial-like conditions (Cutler et al., 2003). At Manning, only two corals have interglacial ages, both of which are from the Holocene (Fig. 4). At the first order, therefore, it appears that glacial conditions are most conducive to coral growth at these two sites.

An enlargement of the age distribution from the last glacial maximum (LGM) through to the Holocene shows pulses of population density. There are no corals from the Last Glacial Maximum [(23–19 ka as defined by the EPILOG working group (Mix et al., 2001)] and there are distinct increases in the number of corals at about 16.5 ka and 12.5 ka (Fig. 4B). In addition, there are increases in population density at around 44 ka and 40 ka (Fig. 6). The first of these pulses (44 ka) is well characterized by ages from the “slab” depicted in Figure 5. The *D. dianthus* corals growing on the gorgonian have a wide range of ages (65–30 ka) but 13 out of the 19 dated corals have ages between 44–42.5 ka.

The last glacial period and the subsequent deglaciation was characterized by unstable climate conditions compared to the Holocene (Grootes et al., 1993; Hughen et



Table 1. Uranium series data summary of concentrations and isotopic ratios. Calculated ages are reported before and after the <sup>230</sup>Th<sub>initial</sub> correction, and are in years before date of analysis (2004). Those samples in bold and marked by an asterisk are within 7% of the modern-day δ<sup>234</sup>U<sub>initial</sub> seawater value (146‰). Database ID is a unique identifier for each deep-sea coral consisting of the Alvin dive, time of collection, station number and individual coral sample. All errors are 2 SE and are reported in unlabeled columns after each value. All corals are *D. dianthus* unless marked; C = *Caryophyllia*, E = *Enalltopsanmia*, S = *Solenastrea*, and Go = *Gorgonian*. Analyses made on the gorgonian coral that forms “The slab” are italicized. Shading highlights replicate measurements from the same coral individual.

| Lab ID | Database ID                           | Smt.  | Depth<br>(m) | 238U<br>(ppm) | 230Th<br>(ppt) | 232Th<br>(ppb) | δ <sup>234</sup><br>U <sub>present</sub><br>‰ | ( <sup>230</sup> Th/<br><sup>238</sup> U)<br>activity | Raw age<br>(yrs) | Corr age<br>(yrs) | U <sub>initial</sub><br>‰ |        |        |     |        |        |       |     |
|--------|---------------------------------------|-------|--------------|---------------|----------------|----------------|---|---|------------------|-------------------|---------------------------|--------|--------|-----|--------|--------|-------|-----|
| UAG01  | <b>ALV-3905-BEAR-112-SS02 (bag 1)</b> | Bear  | 2,165        | 3,522         | 0.001 31.39    | 0.13           | 8,220   | 0.438   | 124.4            | 1.2               | 0.5446                    | 0.0023 | 71,255 | 442 | 69,182 | 2,059  | 151.2 | 1.7 |
| UAG03  | ALV-3905-BEAR-112-SS03 (bag 1)        | Bear  | 2,165        | 3,444         | 0.001 31.37    | 0.13           | 25,869  | 0.435   | 128.7            | 1.2               | 0.5565                    | 0.0024 | 73,020 | 458 | 66,443 | 6,130  | 155.3 | 3.1 |
| UAF19  | ALV-3905-BEAR-112(S)                  | Bear  | 2,165        | 2,830         | 0.002 27.73    | 0.12           | 40,529  | 0.177   | 129.4            | 1.1               | 0.5988                    | 0.0026 | 80,991 | 531 | 67,945 | 11,434 | 156.8 | 5.3 |
| UAJ05  | <b>ALV-3891-1459-003-002*</b>         | Gregg | 1,176        | 4,496         | 0.002 8.39     | 0.04           | 0.878   | 0.006   | 139.6            | 1.1               | 0.1140                    | 0.0005 | 11,486 | 55  | 11,378 | 118    | 144.2 | 1.1 |
| UAJ11  | <b>ALV-3891-1459-003-004*</b>         | Gregg | 1,176        | 3,766         | 0.003 8.71     | 0.04           | 3.214   | 0.015   | 142.6            | 1.2               | 0.1413                    | 0.0007 | 14,379 | 74  | 13,906 | 461    | 148.3 | 1.2 |
| UAM07  | <b>ALV-3891-1459-003-006-001* C</b>   | Gregg | 1,176        | 4,116         | 0.002 8.65     | 0.04           | 2,499   | 0.016   | 143.8            | 1.2               | 0.1284                    | 0.0006 | 12,971 | 63  | 12,638 | 328    | 149.1 | 1.2 |
| UAM08  | <b>ALV-3891-1459-003-006-002* C</b>   | Gregg | 1,176        | 4,682         | 0.002 9.25     | 0.04           | 3.551   | 0.019   | 144.8            | 1.1               | 0.1207                    | 0.0005 | 12,135 | 58  | 11,724 | 400    | 149.7 | 1.2 |
| UAM05  | <b>ALV-3891-1459-003-007*</b>         | Gregg | 1,176        | 4,188         | 0.005 8.08     | 0.04           | 1.617   | 0.022   | 144.9            | 1.4               | 0.1178                    | 0.0005 | 11,833 | 58  | 11,623 | 212    | 149.7 | 1.4 |
| UAM04  | ALV-3891-1459-003-009                 | Gregg | 1,176        | 3,636         | 0.003 9.69     | 0.04           | 1.925   | 0.015   | 150.1            | 1.2               | 0.1629                    | 0.0007 | 16,626 | 81  | 16,327 | 302    | 157.1 | 1.3 |
| UAO19  | ALV-3891-1459-003-009                 | Gregg | 1,176        | 3,605         | 0.002 9.36     | 0.04           | 0.655   | 0.019   | 157.0            | 1.1               | 0.1587                    | 0.0007 | 16,059 | 77  | 15,960 | 123    | 164.3 | 1.1 |
| UAM06  | <b>ALV-3891-1459-003-011*</b>         | Gregg | 1,176        | 3,617         | 0.002 0.22     | 0.00           | 0.292   | 0.011   | 148.2            | 1.1               | 0.0037                    | 0.0000 | 354    | 2   | 315    | 35     | 148.3 | 1.1 |
| UAL05  | <b>ALV-3891-1459-003-013*</b>         | Gregg | 1,176        | 3,734         | 0.002 3.99     | 0.02           | 1.290   | 0.010   | 141.7            | 1.1               | 0.0654                    | 0.0003 | 6,430  | 30  | 6,251  | 176    | 144.3 | 1.2 |
| UAF18  | <b>ALV-3891-1459-003-B5* S</b>        | Gregg | 1,176        | 3,330         | 0.002 0.07     | 0.00           | 0.390   | 0.012   | 149.2            | 1.2               | 0.0014                    | 0.0000 | 130    | 3   | 75     | 32     | 149.3 | 1.2 |
| UAK16  | <b>ALV-3891-1546-004-003*</b>         | Gregg | 1,180        | 3,582         | 0.002 3.27     | 0.01           | 5.171   | 0.023   | 147.5            | 1.1               | 0.0557                    | 0.0002 | 5,430  | 25  | 4,698  | 635    | 149.5 | 1.1 |
| UAA6   | <b>ALV-3891-1646-004-004*</b>         | Gregg | 1,180        | 3,833         | 0.008 9.60     | 0.04           | 5.648   | 0.024   | 144.8            | 3.0               | 0.1530                    | 0.0007 | 15,618 | 92  | 14,830 | 753    | 151.0 | 3.2 |
| UAL14  | <b>ALV-3891-1646-004-004*</b>         | Gregg | 1,180        | 4,921         | 0.004 12.04    | 0.05           | 1.496   | 0.015   | 144.8            | 1.1               | 0.1495                    | 0.0007 | 15,242 | 75  | 15,071 | 182    | 151.1 | 1.1 |
| UAB16  | <b>ALV-3891-1725-005-007*</b>         | Gregg | 1,222        | 3,719         | 0.002 18.84    | 0.09           | 14,614  | 0.064   | 135.5            | 1.1               | 0.3095                    | 0.0015 | 34,517 | 208 | 32,034 | 2,328  | 148.4 | 1.5 |
| UAB17  | <b>ALV-3891-1725-005-007*</b>         | Gregg | 1,222        | 3,728         | 0.002 18.31    | 0.09           | 2,848   | 0.013   | 136.4            | 1.1               | 0.3001                    | 0.0015 | 33,269 | 197 | 32,783 | 510    | 149.7 | 1.2 |
| UAB18  | <b>ALV-3891-1725-005-007*</b>         | Gregg | 1,222        | 4,039         | 0.003 19.81    | 0.10           | 1,817   | 0.008   | 139.6            | 1.1               | 0.2996                    | 0.0015 | 33,093 | 195 | 32,805 | 337    | 153.2 | 1.2 |
| UAB20  | <b>ALV-3891-1725-005-007*</b>         | Gregg | 1,222        | 3,852         | 0.002 18.88    | 0.09           | 2,430   | 0.011   | 135.2            | 1.0               | 0.2995                    | 0.0014 | 33,232 | 194 | 32,829 | 435    | 148.3 | 0.2 |
| UAL10  | ALV-3891-1725-005-007                 | Gregg | 1,222        | 3,734         | 0.002 18.38    | 0.08           | 3,722   | 0.018   | 143.5            | 1.1               | 0.3008                    | 0.0013 | 33,108 | 172 | 32,455 | 657    | 157.3 | 1.2 |
| UAJ09  | <b>ALV-3891-1758-006-003*</b>         | Gregg | 1,221        | 3,665         | 0.002 6.92     | 0.03           | 0.797   | 0.008   | 140.7            | 1.1               | 0.1153                    | 0.0006 | 11,612 | 61  | 11,492 | 131    | 145.4 | 1.1 |
| UAJ05  | <b>ALV-3891-1758-006-006*</b>         | Gregg | 1,221        | 3,676         | 0.002 7.02     | 0.03           | 5,229   | 0.023   | 140.5            | 1.3               | 0.1167                    | 0.0005 | 11,764 | 57  | 10,995 | 721    | 144.9 | 1.3 |
| UAJ07  | <b>ALV-3891-1758-006-007*</b>         | Gregg | 1,221        | 4,058         | 0.002 9.42     | 0.04           | 0.785   | 0.006   | 143.4            | 1.1               | 0.1419                    | 0.0006 | 14,428 | 71  | 14,319 | 127    | 149.3 | 1.1 |

Table 1. Continued.

| Lab ID | Database ID                  | Smt.    | Depth<br>(m) | 238U<br>(ppm) | 230Th<br>(ppt) | 232Th<br>(ppb) | $\frac{^{230}\text{Th}}{^{238}\text{U}}$<br>( $\frac{\text{ppb}}{\text{ppm}}$ ) | $\frac{^{230}\text{Th}}{^{238}\text{U}}$<br>( $\frac{\text{ppb}}{\text{ppm}}$ ) | $\frac{^{230}\text{Th}}{^{238}\text{U}}$<br>( $\frac{\text{ppb}}{\text{ppm}}$ ) | Raw age<br>(yrs) | Corr age<br>(yrs) | $\delta^{234}\text{U}$<br>‰ | $\delta^{234}\text{U}$<br>‰ |         |       |         |       |       |     |
|--------|------------------------------|---------|--------------|---------------|----------------|----------------|---|---|---|------------------|-------------------|-----------------------------|-----------------------------|---------|-------|---------|-------|-------|-----|
| UAG02  | ALV-3904-KEL-201/202 SS02*   | Kelvin  | 1,670        | 3.345         | 0.001          | 18.91          | 0.08  | 0.432   | 1.049   | 132.6            | 1.3               | 0.3455                      | 0.0015                      | 39,432  | 212   | 39,338  | 228   | 148.2 | 1.4 |
| UAG04  | ALV-3904-KEL-201/202 SS03*   | Kelvin  | 1,670        | 2.432         | 0.001          | 13.79          | 0.06  | 0.437   | 1.093   | 131.6            | 1.1               | 0.3464                      | 0.0015                      | 39,610  | 212   | 39,483  | 242   | 147.1 | 1.3 |
| UAF16  | ALV-3883-1248-003-003 S*     | Manning | 1,524        | 4.632         | 0.002          | 0.11           | 0.00  | 0.171   | 0.006   | 148.9            | 1.2               | 0.0014                      | 0.0000                      | 135     | 1     | 118     | 15    | 148.9 | 1.2 |
| UAA7   | ALV-3883-1248-003-004*       | Manning | 1,524        | 3.531         | 0.008          | 22.56          | 0.10  | 5.145   | 0.022   | 129.4            | 3.0               | 0.3903                      | 0.0019                      | 45,895  | 318   | 44,859  | 1,055 | 146.9 | 3.5 |
| UAA1   | ALV-3883-1346-004-003*       | Manning | 1,506        | 3.836         | 0.008          | 26.35          | 0.11  | 8.752   | 0.037   | 127.1            | 3.0               | 0.4198                      | 0.0020                      | 50,383  | 352   | 48,700  | 1,662 | 145.9 | 3.5 |
| UAE04  | ALV-3890-1235-001-002        | Manning | 2,004        | 3.522         | 0.002          | 20.52          | 0.09  | 1.019   | 0.004   | 139.2            | 5.0               | 0.3559                      | 0.0015                      | 40,571  | 309   | 40,361  | 366   | 156.0 | 5.6 |
| UAH02  | ALV-3890-1235-001-003*       | Manning | 2,004        | 4.743         | 0.003          | 37.70          | 0.18  | 4.342   | 0.021   | 122.2            | 1.2               | 0.4856                      | 0.0023                      | 61,171  | 394   | 60,383  | 861   | 144.9 | 1.4 |
| UAG14  | ALV-3890-1330-002-003        | Manning | 1,886        | 2.951         | 0.002          | 23.73          | 0.10  | 9.609   | 0.442   | 143.6            | 1.2               | 0.4914                      | 0.0022                      | 60,488  | 367   | 57,920  | 2,496 | 169.1 | 1.8 |
| UAG05  | ALV-3890-1330-002-004*       | Manning | 1,886        | 4.162         | 0.003          | 11.38          | 0.05  | 4.537   | 0.484   | 143.4            | 1.1               | 0.1670                      | 0.0007                      | 17,187  | 85    | 16,594  | 577   | 150.3 | 1.2 |
| UAG07  | ALV-3890-1330-002-005        | Manning | 1,886        | 2.796         | 0.001          | 39.20          | 0.17  | 2.000   | 0.533   | 115.7            | 1.2               | 0.8567                      | 0.0038                      | 152,707 | 1,483 | 151,351 | 1,957 | 177.4 | 2.1 |
| UAE19  | ALV-3890-1330-002-006        | Manning | 1,886        | 3.161         | 0.002          | 43.74          | 0.19  | 1.225   | 0.005   | 117.6            | 1.2               | 0.8456                      | 0.0038                      | 147,988 | 1,410 | 147,233 | 1,566 | 178.3 | 1.9 |
| UAG06  | ALV-3890-1330-002-007*       | Manning | 1,886        | 3.640         | 0.002          | 9.52           | 0.04  | 1.567   | 0.580   | 142.2            | 1.1               | 0.1597                      | 0.0007                      | 16,399  | 79    | 16,164  | 242   | 148.8 | 1.2 |
| UAG20  | ALV-3890-1330-002-008        | Manning | 1,886        | 3.806         | 0.002          | 10.33          | 0.05  | 3.767   | 0.500   | 150.1            | 1.2               | 0.1659                      | 0.0007                      | 16,955  | 84    | 16,420  | 523   | 157.2 | 1.3 |
| UAE16  | ALV-3890-1407-003-001*       | Manning | 1,778        | 3.361         | 0.002          | 6.84           | 0.03  | 1.888   | 0.008   | 144.8            | 1.1               | 0.1244                      | 0.0006                      | 12,528  | 65    | 12,222  | 304   | 149.9 | 1.1 |
| UAG12  | ALV-3890-1407-003-003*       | Manning | 1,778        | 3.488         | 0.002          | 9.18           | 0.04  | 0.866   | 0.775   | 145.9            | 1.1               | 0.1609                      | 0.0007                      | 16,467  | 81    | 16,331  | 155   | 152.8 | 1.2 |
| UAG13  | ALV-3890-1407-003-003*       | Manning | 1,778        | 3.579         | 0.002          | 9.42           | 0.04  | 2.138   | 0.564   | 143.2            | 1.1               | 0.1608                      | 0.0007                      | 16,505  | 82    | 16,181  | 326   | 149.9 | 1.2 |
| UAF17  | ALV-3890-1642-005-B6 E       | Manning | 1,487        | 4.113         | 0.003          | 19.43          | 0.08  | 3.044   | 0.022   | 149.1            | 1.2               | 0.2887                      | 0.0013                      | 31,392  | 164   | 30,934  | 474   | 162.7 | 1.3 |
| UAK04  | ALV-3890-1643-005-0002 lower | Manning | 1,487        | 3.436         | 0.002          | 9.99           | 0.04  | 0.753   | 0.017   | 150.6            | 1.1               | 0.1777                      | 0.0008                      | 18,254  | 89    | 18,127  | 152   | 158.5 | 1.2 |
| UAK03  | ALV-3890-1643-005-0002 upper | Manning | 1,487        | 3.968         | 0.002          | 11.10          | 0.05  | 1.185   | 0.014   | 149.4            | 1.0               | 0.1709                      | 0.0007                      | 17,521  | 85    | 17,350  | 187   | 156.9 | 1.1 |
| UAJ06  | ALV-3890-1643-005-001*       | Manning | 1,487        | 3.950         | 0.002          | 9.60           | 0.04  | 1.900   | 0.014   | 132.6            | 1.1               | 0.1485                      | 0.0006                      | 15,301  | 74    | 15,028  | 275   | 138.3 | 1.2 |
| UAL06  | ALV-3890-1643-005-003        | Manning | 1,487        | 3.459         | 0.002          | 9.48           | 0.04  | 0.563   | 0.015   | 148.5            | 1.1               | 0.1675                      | 0.0007                      | 17,158  | 83    | 17,064  | 123   | 155.8 | 1.2 |
| UAE15  | ALV-3890-1643-005-004*       | Manning | 1,487        | 3.718         | 0.002          | 29.11          | 0.13  | 0.438   | 0.002   | 128.8            | 1.2               | 0.4784                      | 0.0022                      | 59,471  | 365   | 59,360  | 377   | 152.4 | 1.4 |
| UAE17  | ALV-3890-1643-005-005*       | Manning | 1,487        | 3.429         | 0.001          | 4.06           | 0.02  | 0.436   | 0.002   | 135.5            | 1.1               | 0.0724                      | 0.0003                      | 7,187   | 35    | 7,120   | 74    | 138.3 | 1.1 |
| UAJ02  | ALV-3890-1643-005-006        | Manning | 1,487        | 3.282         | 0.002          | 25.57          | 0.11  | 1.242   | 0.011   | 132.6            | 1.1               | 0.4759                      | 0.0021                      | 58,796  | 344   | 58,472  | 462   | 156.4 | 1.4 |
| UAF15  | ALV-3890-1643-005-B4 F*      | Manning | 1,487        | 4.073         | 0.002          | 0.17           | 0.00  | 0.362   | 0.006   | 143.4            | 1.1               | 0.0026                      | 0.0000                      | 248     | 2     | 207     | 35    | 143.5 | 1.1 |
| UAE05  | ALV-3890-1718-006-001*       | Manning | 1,421        | 3.267         | 0.004          | 2.36           | 0.01  | 2.132   | 0.009   | 149.6            | 5.0               | 0.0441                      | 0.0002                      | 4,272   | 28    | 39,44   | 304   | 151.3 | 5.1 |

Table 1. Continued.

| Lab ID                          | Database ID               | Smt.    | Depth (m) | <sup>238</sup> U (ppm) | <sup>230</sup> Th (ppt) | <sup>232</sup> Th (ppb) | $\frac{^{230}\text{Th}}{^{238}\text{U}}$ (mean %C) | $\frac{^{230}\text{Th}}{^{238}\text{U}}$ activity | Raw age (yrs) | Corr age (yrs) | $\delta^{234}\text{U}$ (‰) |        |        |        |     |        |     |       |     |
|---------------------------------|---------------------------|---------|-----------|------------------------|-------------------------|-------------------------|--|---|---------------|----------------|----------------------------|--------|--------|--------|-----|--------|-----|-------|-----|
| UA007                           | ALV-3890-1742-007-001*    | Manning | 1,381     | 4.292                  | 0.002                   | 11.14                   | 0.05   | 2.975   | 0.013         | 146.0          | 1.1                        | 0.1586 | 0.0007 | 16,215 | 78  | 15,825 | 386 | 152.7 | 1.2 |
| UA020                           | ALV-3890-1742-007-002     | Manning | 1,381     | 3.039                  | 0.002                   | 8.05                    | 0.03   | 0.987   | 0.007         | 148.4          | 1.1                        | 0.1619 | 0.0007 | 16,536 | 80  | 16,351 | 196 | 155.4 | 1.2 |
| UA008                           | ALV-3892-1315-001-002*    | Manning | 1,713     | 3.143                  | 0.001                   | 16.86                   | 0.07   | 0.405   | 0.002         | 134.9          | 4.0                        | 0.3278 | 0.0014 | 36,951 | 251 | 36,860 | 263 | 149.7 | 4.5 |
| UA009                           | ALV-3892-1315-001-003*    | Manning | 1,713     | 3.829                  | 0.002                   | 10.08                   | 0.04   | 2.548   | 0.011         | 143.5          | 1.2                        | 0.1609 | 0.0007 | 16,509 | 79  | 16,133 | 374 | 150.2 | 1.2 |
| UA016                           | ALV-3892-1315-001-003     | Manning | 1,713     | 4.031                  | 0.002                   | 10.28                   | 0.05   | 0.694   | 0.017         | 148.7          | 1.1                        | 0.1558 | 0.0007 | 15,868 | 80  | 15,773 | 121 | 155.5 | 1.1 |
| UA005                           | ALV-3892-1315-001-006     | Manning | 1,713     | 3.284                  | 0.002                   | 16.82                   | 0.07   | 1.185   | 0.014         | 140.9          | 1.1                        | 0.3129 | 0.0014 | 34,757 | 181 | 34,512 | 297 | 155.3 | 1.2 |
| UA011                           | ALV-3892-1315-001-007*    | Manning | 1,713     | 6.668                  | 0.004                   | 27.07                   | 0.12   | 8.491   | 0.036         | 137.2          | 1.2                        | 0.2481 | 0.0011 | 26,736 | 139 | 25,977 | 746 | 147.6 | 1.3 |
| UA012                           | ALV-3892-1315-001-007*    | Manning | 1,713     | 6.683                  | 0.005                   | 26.86                   | 0.12   | 9.705   | 0.043         | 129.4          | 4.0                        | 0.2456 | 0.0011 | 26,651 | 177 | 25,781 | 856 | 139.2 | 4.3 |
| UA013                           | ALV-3892-1315-001-007*    | Manning | 1,713     | 6.520                  | 0.003                   | 26.34                   | 0.11   | 8.511   | 0.036         | 136.0          | 1.0                        | 0.2469 | 0.0011 | 26,625 | 137 | 25,848 | 755 | 146.4 | 1.1 |
| UA014                           | ALV-3892-1315-001-007*    | Manning | 1,713     | 6.607                  | 0.003                   | 26.46                   | 0.13   | 8.492   | 0.037         | 134.1          | 1.0                        | 0.2447 | 0.0012 | 26,410 | 150 | 25,644 | 755 | 144.2 | 1.2 |
| UA015                           | ALV-3892-1315-001-007*    | Manning | 1,713     | 6.409                  | 0.003                   | 25.92                   | 0.12   | 8.325   | 0.036         | 134.5          | 1.1                        | 0.2471 | 0.0011 | 26,690 | 146 | 25,915 | 763 | 144.7 | 1.2 |
| UA017                           | ALV-3892-1315-001-007*    | Manning | 1,713     | 6.695                  | 0.003                   | 26.82                   | 0.12   | 10.268  | 0.044         | 135.0          | 1.0                        | 0.2475 | 0.0011 | 26,393 | 132 | 25,444 | 922 | 145.0 | 1.2 |
| UA015                           | ALV-3892-1315-001-007*    | Manning | 1,713     | 4.540                  | 0.002                   | 17.65                   | 0.08   | 3.234   | 0.019         | 136.0          | 1.0                        | 0.2375 | 0.0010 | 25,496 | 128 | 25,073 | 431 | 146.0 | 1.2 |
| UA003                           | ALV-3892-1315-001-008*    | Manning | 1,713     | 3.516                  | 0.002                   | 9.05                    | 0.04   | 1.396   | 0.006         | 142.1          | 4.0                        | 0.1572 | 0.0007 | 16,123 | 99  | 15,906 | 232 | 148.6 | 4.2 |
| UA016                           | ALV-3892-1315-001-008*    | Manning | 1,713     | 3.525                  | 0.002                   | 9.15                    | 0.04   | 0.756   | 0.007         | 142.4          | 1.1                        | 0.1586 | 0.0007 | 16,268 | 78  | 16,145 | 142 | 149.1 | 1.1 |
| UA001                           | ALV-3892-1315-001-010*    | Manning | 1,713     | 4.712                  | 0.002                   | 21.83                   | 0.09   | 0.535   | 0.002         | 128.1          | 4.0                        | 0.2831 | 0.0012 | 31,372 | 207 | 31,296 | 218 | 139.9 | 4.4 |
| UA007                           | ALV-3892-1315-001-B4-SS1  | Manning | 1,713     | 3.120                  | 0.002                   | 9.28                    | 0.04   | 0.905   | 0.012         | 149.2          | 1.1                        | 0.1817 | 0.0008 | 18,726 | 91  | 18,557 | 187 | 157.2 | 1.1 |
| UA008                           | ALV-3892-1315-001-B4-SS2  | Manning | 1,713     | 3.862                  | 0.002                   | 8.50                    | 0.04   | 0.713   | 0.014         | 149.4          | 1.1                        | 0.1344 | 0.0006 | 13,549 | 64  | 13,446 | 119 | 155.2 | 1.1 |
| UA009                           | ALV-3892-1315-001-B4-SS3* | Manning | 1,713     | 3.622                  | 0.002                   | 9.41                    | 0.04   | 0.684   | 0.008         | 142.8          | 1.2                        | 0.1587 | 0.0007 | 16,273 | 81  | 16,164 | 133 | 149.5 | 1.2 |
| UA007                           | ALV-3892-1711-006-002     | Manning | 1,548     | 3.181                  | 0.003                   | 24.49                   | 0.11   | 2.157   | 0.009         | 136.8          | 4.1                        | 0.4704 | 0.0022 | 57,607 | 450 | 57,068 | 685 | 160.7 | 4.8 |
| UA002                           | ALV-3892-1711-006-004*    | Manning | 1,548     | 3.687                  | 0.003                   | 21.08                   | 0.09   | 0.929   | 0.004         | 134.3          | 4.0                        | 0.3493 | 0.0016 | 39,880 | 278 | 39,704 | 323 | 150.3 | 4.5 |
| UA004                           | ALV-3892-1711-006-006     | Manning | 1,548     | 3.331                  | 0.003                   | 25.63                   | 0.11   | 1.544   | 0.007         | 135.0          | 4.0                        | 0.4701 | 0.0021 | 57,686 | 446 | 57,313 | 569 | 158.7 | 4.8 |
| UA010                           | ALV-3892-1711-006-008     | Manning | 1,548     | 3.384                  | 0.002                   | 19.37                   | 0.09   | 0.808   | 0.003         | 140.2          | 4.0                        | 0.3496 | 0.0016 | 36,951 | 256 | 36,860 | 318 | 156.7 | 4.5 |
| UA006                           | ALV-3892-1711-006-010*    | Manning | 1,548     | 3.250                  | 0.003                   | 18.64                   | 0.08   | 0.943   | 0.004         | 133.0          | 4.0                        | 0.3505 | 0.0016 | 40,099 | 282 | 39,896 | 340 | 148.9 | 4.5 |
| From the fallen gorgonian coral |                           |         |           |                        |                         |                         |  |   |               |                |                            |        |        |        |     |        |     |       |     |
| UA001a                          | ALV-3892-1421-002-001-05* | Manning | 1,657     | 4.263                  | 0.003                   | 26.61                   | 0.11   | 1.502   | 0.007         | 130.4          | 5.0                        | 0.3814 | 0.0017 | 44,549 | 350 | 44,284 | 430 | 147.8 | 5.7 |

Table 1. Continued.

| Lab ID | Database ID                  | Smt.    | Depth<br>(m) | 238U<br>(ppm) | 230Th<br>(ppt) | 232Th<br>(pnb) | $\delta^{234}\text{U}$<br>$\frac{U_{234}}{U_{238}}$<br>‰ | $\frac{(^{230}\text{Th}/^{232}\text{Th})}{\text{activity}}$ | Raw age<br>(yrs) | Corr age<br>(yrs) | $\delta^{234}\text{U}$<br>$\frac{U_{\text{initial}}}{U_{\text{final}}}$<br>‰ |        |        |         |       |         |       |       |      |
|--------|------------------------------|---------|--------------|---------------|----------------|----------------|--|---|------------------|-------------------|--|--------|--------|---------|-------|---------|-------|-------|------|
| UAD001 | ALV-3892-1421-002-001-06*    | Manning | 1,657        | 3,246         | 0.002          | 19.64          | 0.18   | 0.500   | 0.024            | 130.0             | 4.0  | 0.3697 | 0.0033 | 42,918  | 509   | 42,799  | 519   | 146.8 | 4.5  |
| UAD002 | ALV-3892-1421-002-001-07*    | Manning | 1,657        | 4,070         | 0.002          | 18.22          | 0.12   | 0.492   | 0.015            | 130.6             | 4.0  | 0.2735 | 0.0018 | 30,074  | 265   | 29,991  | 275   | 142.1 | 4.4  |
| UAD003 | ALV-3892-1421-002-001-08*    | Manning | 1,657        | 2,815         | 0.002          | 16.99          | 0.16   | 0.296   | 0.023            | 133.4             | 4.0  | 0.3688 | 0.0035 | 42,624  | 532   | 42,541  | 536   | 150.4 | 4.5  |
| UAD004 | ALV-3892-1421-002-001-09*    | Manning | 1,657        | 4,419         | 0.003          | 27.16          | 0.22   | 3.412   | 0.032            | 126.1             | 4.0  | 0.3756 | 0.0030 | 43,943  | 475   | 43,374  | 725   | 142.5 | 4.6  |
| UAD005 | ALV-3892-1421-002-001-10*    | Manning | 1,657        | 3,564         | 0.002          | 21.88          | 0.10   | 0.468   | 0.002            | 135.2             | 4.0  | 0.3752 | 0.0017 | 43,432  | 307   | 43,329  | 319   | 152.9 | 4.5  |
| UAD006 | ALV-3892-1421-002-001-11     | Manning | 1,657        | 3,486         | 0.002          | 21.45          | 0.09   | 0.875   | 0.004            | 136.2             | 4.0  | 0.3761 | 0.0016 | 43,509  | 304   | 43,321  | 351   | 154.0 | 4.5  |
| UAD007 | ALV-3892-1421-002-001-12*    | Manning | 1,657        | 4,442         | 0.002          | 27.64          | 0.12   | 2.253   | 0.010            | 131.6             | 4.0  | 0.3803 | 0.0017 | 44,332  | 314   | 43,956  | 479   | 149.0 | 4.6  |
| UAD008 | ALV-3892-1421-002-001-13*    | Manning | 1,657        | 4,394         | 0.002          | 27.20          | 0.12   | 1.731   | 0.007            | 135.2             | 4.0  | 0.3782 | 0.0017 | 43,857  | 308   | 43,565  | 415   | 152.9 | 4.5  |
| UAD009 | ALV-3892-1421-002-001-14*    | Manning | 1,657        | 3,796         | 0.001          | 23.53          | 0.11   | 0.529   | 0.002            | 134.1             | 4.0  | 0.3787 | 0.0018 | 43,982  | 323   | 43,873  | 336   | 151.8 | 4.5  |
| UAD010 | ALV-3892-1421-002-001-15*    | Manning | 1,657        | 3,429         | 0.001          | 21.16          | 0.10   | 0.874   | 0.004            | 127.6             | 4.0  | 0.3771 | 0.0017 | 44,075  | 319   | 43,881  | 366   | 144.5 | 4.5  |
| UAD011 | ALV-3892-1421-002-001-16*    | Manning | 1,657        | 3,577         | 0.002          | 22.33          | 0.16   | 1.390   | 0.007            | 132.2             | 4.0  | 0.3814 | 0.0027 | 44,464  | 436   | 44,174  | 515   | 149.8 | 4.6  |
| UAD012 | ALV-3892-1421-002-001-17*    | Manning | 1,657        | 3,506         | 0.002          | 22.97          | 0.25   | 0.562   | 0.004            | 134.3             | 4.0  | 0.4003 | 0.0044 | 47,078  | 681   | 46,950  | 689   | 153.4 | 4.6  |
| UAD013 | ALV-3892-1421-002-001-18*    | Manning | 1,657        | 3,460         | 0.002          | 21.40          | 0.09   | 0.631   | 0.003            | 123.9             | 4.0  | 0.3779 | 0.0016 | 44,385  | 313   | 44,243  | 338   | 140.4 | 4.6  |
| UAD015 | ALV-3892-1421-002-001-20*    | Manning | 1,657        | 3,091         | 0.002          | 23.24          | 0.10   | 1.233   | 0.005            | 139.9             | 4.0  | 0.4594 | 0.0020 | 55,662  | 417   | 55,334  | 519   | 163.6 | 4.7  |
| UAE02  | ALV-3892-1421-002-001-20*    | Manning | 1,657        | 3,214         | 0.003          | 24.30          | 0.11   | 0.705   | 0.003            | 130.3             | 5.0  | 0.4620 | 0.0021 | 56,719  | 482   | 56,529  | 509   | 152.9 | 5.9  |
| UAD20  | ALV-3892-1421-002-001-25*    | Manning | 1,657        | 3,730         | 0.002          | 31.48          | 0.14   | 1.696   | 0.007            | 126.7             | 4.0  | 0.5156 | 0.0022 | 65,900  | 518   | 65,485  | 649   | 152.4 | 4.8  |
| UAD14  | ALV-3892-1421-002-001-19 Go  | Manning | 1,657        | 1,151         | 0.000          | 0.78           | 0.00   | 0.131   | 0.001            | 142.4             | 4.3  | 0.3172 | 0.0018 | 35,270  | 292   | 34,686  | 636   | 157.1 | 4.8  |
| UAD16  | ALV-3892-1421-002-001-21 Go* | Manning | 1,657        | 0,094         | 0.000          | 0.58           | 0.01   | 0.660   | 0.003            | 135.5             | 4.1  | 0.3813 | 0.0082 | 44,287  | 1,192 | 39,292  | 4,630 | 151.4 | 5.0  |
| UAD17  | ALV-3892-1421-002-001-22 Go  | Manning | 1,657        | 1,186         | 0.000          | 1.00           | 0.02   | 0.418   | 0.002            | 161.0             | 4.1  | 0.3294 | 0.0081 | 36,146  | 1,061 | 34,673  | 1,742 | 177.5 | 4.6  |
| UAD18  | ALV-3892-1421-002-001-23 Go  | Manning | 1,657        | 1,154         | 0.000          | 0.82           | 0.02   | 0.049   | 0.001            | 154.6             | 4.0  | 0.3262 | 0.0071 | 35,975  | 939   | 35,757  | 956   | 171.1 | 4.5  |
| UAD19  | ALV-3892-1421-002-001-24 Go  | Manning | 1,657        | 1,146         | 0.000          | 0.98           | 0.06   | 0.083   | 0.001            | 162.2             | 4.1  | 0.4109 | 0.0269 | 47,109  | 3,887 | 46,691  | 3,867 | 185.1 | 5.1  |
| UAE11  | ALV-3884-1411-002-104*       | Muir    | 2,228        | 3,199         | 0.002          | 8.28           | 0.04   | 1.659   | 0.007            | 142.6             | 1.1  | 0.1581 | 0.0007 | 16,218  | 79    | 15,925  | 296   | 149.2 | 1.2  |
| UAF08  | ALV-3884-1531-002-013*       | Muir    | 2,228        | 3,383         | 0.002          | 8.42           | 0.04   | 0.339   | 0.011            | 140.2             | 1.1  | 0.1521 | 0.0007 | 15,586  | 75    | 15,530  | 92    | 146.5 | 1.1  |
| UAJ17  | ALV-3884-1531-003-008*       | Muir    | 2,141        | 3,700         | 0.003          | 9.24           | 0.04   | 2.201   | 0.016            | 145.5             | 1.2  | 0.1526 | 0.0007 | 15,571  | 77    | 15,237  | 333   | 151.9 | 1.3  |
| UAE13  | ALV-3884-1531-003-011*       | Muir    | 2,141        | 2,859         | 0.002          | 46.82          | 0.20   | 3.189   | 0.014            | 111.0             | 5.0  | 1.0008 | 0.0043 | 229,510 | 5,302 | 225,285 | 6,417 | 209.9 | 10.1 |
| UAJ19  | ALV-3884-1638-004-014*       | Muir    | 2,084        | 3,836         | 0.003          | 9.95           | 0.04   | 0.927   | 0.008            | 140.0             | 1.1  | 0.1584 | 0.0007 | 16,288  | 80    | 16,149  | 157   | 146.6 | 1.2  |

Table 1. Continued.

| Lab ID | Database ID                 | Smt. | Depth<br>(m) | 238U<br>(ppm) | 230Th<br>(ppt) | 232Th<br>(ppb) | $\delta^{234}$<br>U<br>‰ | $(^{230}\text{Th}/^{238}\text{U})$<br>activity | Raw age<br>(yrs) | Corr age<br>(yrs) | $\delta^{234}$<br>U<br>‰ |        |        |         |        |         |       |       |     |
|--------|-----------------------------|------|--------------|---------------|----------------|----------------|--------------------------|--|------------------|-------------------|--------------------------|--------|--------|---------|--------|---------|-------|-------|-----|
| UAEl2  | ALV-3884-1638-004-210*      | Muir | 2,084        | 3.286         | 0.002          | 8.16           | 0.04                     | 0.422  | 0.002            | 141.7             | 1.2                      | 0.1518 | 0.0007 | 75      | 15,458 | 103     | 148.0 | 1.2   |     |
| UA102  | ALV-3885-1239-001-002*      | Muir | 2,027        | 3.507         | 0.002          | 9.99           | 0.05                     | 0.190  | 0.042            | 145.2             | 1.1                      | 0.1741 | 0.0009 | 17,945  | 100    | 16,462  | 1,369 | 152.2 | 1.3 |
| UAG15  | ALV-3885-1239-001-004*      | Muir | 2,027        | 3.416         | 0.002          | 9.10           | 0.04                     | 1.602  | 0.625            | 142.2             | 1.1                      | 0.1627 | 0.0007 | 16,733  | 82     | 16,476  | 263   | 149.0 | 1.2 |
| UAEl0  | ALV-3885-1239-001-007       | Muir | 2,027        | 3.129         | 0.002          | 8.47           | 0.04                     | 3.092  | 0.013            | 146.5             | 1.1                      | 0.1654 | 0.0007 | 16,963  | 82     | 16,405  | 544   | 153.4 | 1.2 |
| UAO17  | ALV-3885-1239-001-007       | Muir | 2,027        | 3.135         | 0.002          | 7.99           | 0.04                     | 0.694  | 0.013            | 146.7             | 1.1                      | 0.1558 | 0.0007 | 15,901  | 78     | 15,780  | 141   | 153.4 | 1.1 |
| UAG08  | ALV-3885-1239-001-011*      | Muir | 2,027        | 2.289         | 0.002          | 5.99           | 0.03                     | 0.672  | 0.989            | 140.6             | 1.1                      | 0.1599 | 0.0007 | 16,438  | 80     | 16,277  | 176   | 147.2 | 1.2 |
| UA103  | ALV-3885-1239-001-012*      | Muir | 2,027        | 3.087         | 0.002          | 8.16           | 0.04                     | 1.793  | 0.010            | 142.1             | 1.1                      | 0.1615 | 0.0008 | 16,598  | 90     | 16,268  | 333   | 148.8 | 1.2 |
| UAO18  | ALV-3885-1239-001-012       | Muir | 2,027        | 3.316         | 0.002          | 8.43           | 0.04                     | 0.882  | 0.013            | 150.6             | 1.1                      | 0.1553 | 0.0007 | 15,781  | 77     | 15,637  | 160   | 157.4 | 1.1 |
| UAEl6  | ALV-3885-1239-001-014*      | Muir | 2,027        | 4.829         | 0.002          | 12.63          | 0.05                     | 1.116  | 0.005            | 142.4             | 1.1                      | 0.1598 | 0.0007 | 16,401  | 79     | 16,268  | 151   | 149.1 | 1.2 |
| UAG11  | ALV-3885-1239-001-015*      | Muir | 2,027        | 3.384         | 0.002          | 8.81           | 0.04                     | 0.735  | 1.214            | 141.6             | 1.1                      | 0.1591 | 0.0007 | 16,343  | 81     | 16,223  | 141   | 148.3 | 1.2 |
| UAEl20 | ALV-3885-1325-002-034*      | Muir | 1,986        | 3.262         | 0.001          | 22.12          | 0.10                     | 1.705  | 0.007            | 130.8             | 1.1                      | 0.4143 | 0.0019 | 49,345  | 284    | 48,939  | 484   | 150.2 | 1.3 |
| UAF06  | ALV-3885-1325-002-039*      | Muir | 1,986        | 3.695         | 0.002          | 24.73          | 0.11                     | 1.184  | 0.012            | 126.0             | 1.2                      | 0.4089 | 0.0018 | 48,815  | 275    | 48,572  | 359   | 144.6 | 1.3 |
| UAF09  | ALV-3885-1420-003-003*      | Muir | 1,929        | 3.634         | 0.002          | 27.95          | 0.12                     | 1.203  | 0.009            | 121.6             | 1.1                      | 0.4699 | 0.0020 | 58,615  | 343    | 58,339  | 431   | 143.4 | 1.3 |
| UAG19  | ALV-3885-1452-004-001*      | Muir | 1,878        | 3.465         | 0.001          | 28.25          | 0.12                     | 4.744  | 0.438            | 127.0             | 1.2                      | 0.4981 | 0.0022 | 62,883  | 378    | 61,746  | 1,168 | 151.2 | 1.5 |
| UAEl4  | ALV-3885-1452-004-003*      | Muir | 1,878        | 3.420         | 0.002          | 26.56          | 0.12                     | 1.651  | 0.007            | 126.6             | 1.2                      | 0.4745 | 0.0022 | 59,005  | 365    | 58,593  | 538   | 149.4 | 1.4 |
| UA101  | ALV-3885-1452-004-007*      | Muir | 1,878        | 3.573         | 0.002          | 24.65          | 0.11                     | 0.987  | 0.010            | 128.1             | 1.2                      | 0.4215 | 0.0018 | 50,574  | 286    | 50,351  | 355   | 147.7 | 1.3 |
| UAF03  | ALV-3885-1452-004-010*      | Muir | 1,878        | 3.353         | 0.002          | 26.60          | 0.11                     | 1.905  | 0.014            | 127.9             | 1.1                      | 0.4847 | 0.0021 | 60,583  | 359    | 60,113  | 578   | 151.6 | 1.4 |
| UAG17  | ALV-3885-1520-005-006       | Muir | 1,821        | 4.437         | 0.002          | 63.94          | 0.30                     | 2.420  | 0.531            | 100.6             | 1.2                      | 0.8805 | 0.0042 | 167,947 | 1,899  | 166,726 | 2,204 | 161.2 | 2.1 |
| UAG10  | ALV-3885-1520-005-007-lower | Muir | 1,821        | 1.138         | 0.002          | 16.31          | 0.07                     | 0.501  | 1.405            | 103.0             | 1.2                      | 0.8761 | 0.0041 | 165,089 | 1,831  | 164,118 | 2,029 | 163.9 | 2.1 |
| UAG09  | ALV-3885-1520-005-007-upper | Muir | 1,821        | 6.698         | 0.004          | 95.63          | 0.42                     | 2.488  | 0.528            | 106.4             | 1.1                      | 0.8723 | 0.0038 | 162,169 | 1,645  | 161,364 | 1,793 | 167.9 | 2.0 |
| UAH06  | ALV-3885-1520-005-008*      | Muir | 1,821        | 3.848         | 0.001          | 26.16          | 0.12                     | 1.448  | 0.008            | 128.0             | 1.1                      | 0.4153 | 0.0019 | 49,656  | 289    | 49,359  | 405   | 147.1 | 1.3 |
| UAG18  | ALV-3885-1520-005-012       | Muir | 1,821        | 4.580         | 0.002          | 66.03          | 0.30                     | 6.045  | 0.448            | 101.0             | 1.2                      | 0.8808 | 0.0040 | 167,944 | 1,823  | 165,097 | 3,290 | 161.1 | 2.4 |
| UAEl8  | ALV-3885-1520-005-014       | Muir | 1,821        | 4.587         | 0.002          | 65.27          | 0.29                     | 2.796  | 0.012            | 100.5             | 1.2                      | 0.8693 | 0.0039 | 163,232 | 1,719  | 161,878 | 2,132 | 158.8 | 2.1 |
| UAG16  | ALV-3885-1739-007-003       | Muir | 1,791        | 2.693         | 0.002          | 42.33          | 0.19                     | 3.676  | 0.477            | 96.9              | 1.1                      | 0.9605 | 0.0042 | 212,243 | 2,896  | 207,902 | 5,063 | 174.5 | 3.2 |
| UA120  | ALV-3887-1324-002-002*      | Muir | 2,546        | 4.330         | 0.002          | 8.82           | 0.04                     | 0.810  | 0.007            | 142.9             | 1.2                      | 0.1244 | 0.0006 | 12,553  | 61     | 12,449  | 117   | 148.1 | 1.2 |
| UAJ20  | ALV-3887-1324-002-005*      | Muir | 2,546        | 4.596         | 0.003          | 9.33           | 0.04                     | 0.572  | 0.008            | 140.9             | 1.1                      | 0.1241 | 0.0006 | 12,545  | 61     | 12,475  | 91    | 145.9 | 1.2 |

Table 1. Continued.

| Lab ID | Database ID            | Smt. | Depth<br>238U<br>(m) | <sup>238</sup> Th<br>(ppb) | <sup>232</sup> Th<br>(ppb) | $\delta^{234}$<br>U <sub>mean</sub><br>‰ | $\frac{(^{230}\text{Th}/^{238}\text{U})}{\text{activity}}$ | Raw age<br>(yrs) | Corr age<br>(yrs) | $\delta^{234}$<br>U <sub>initial</sub><br>‰ |     |        |        |        |     |        |       |       |     |
|--------|------------------------|------|----------------------|----------------------------|----------------------------|--|--|------------------|-------------------|---|-----|--------|--------|--------|-----|--------|-------|-------|-----|
| UA116  | ALV-3887-1436-003-003* | Muir | 2,441                | 3,488                      | 0.002                      | 8.65                                     | 0.04   | 0.657            | 0.010             | 143.5                                       | 1.1 | 0.1515 | 0.0007 | 15,478 | 76  | 15,370 | 129   | 149.8 | 1.2 |
| UA106  | ALV-3887-1436-003-006* | Muir | 2,441                | 3,750                      | 0.001                      | 39.46                                    | 0.17   | 2.076            | 0.010             | 116.6                                       | 1.2 | 0.6430 | 0.0028 | 91,822 | 637 | 91,181 | 882   | 150.9 | 1.6 |
| UAF05  | ALV-3887-1436-003-007* | Muir | 2,441                | 3,296                      | 0.002                      | 32.52                                    | 0.14   | 1.355            | 0.010             | 121.5                                       | 1.1 | 0.6028 | 0.0026 | 82,722 | 552 | 82,297 | 681   | 153.4 | 1.5 |
| UAF04  | ALV-3887-1436-003-010* | Muir | 2,441                | 3,665                      | 0.002                      | 37.74                                    | 0.16   | 0.982            | 0.010             | 118.1                                       | 1.1 | 0.6292 | 0.0027 | 88,626 | 605 | 88,325 | 664   | 151.6 | 1.5 |
| UA119  | ALV-3887-1436-003-011* | Muir | 2,441                | 3,366                      | 0.002                      | 35.36                                    | 0.15   | 4.363            | 0.021             | 117.6                                       | 1.2 | 0.6417 | 0.0028 | 91,400 | 641 | 89,942 | 1,553 | 151.6 | 1.7 |
| UAJ04  | ALV-3887-1549-004-002* | Muir | 2,372                | 3,755                      | 0.002                      | 9.30                                     | 0.04   | 0.474            | 0.004             | 142.1                                       | 1.1 | 0.1513 | 0.0007 | 15,475 | 75  | 15,402 | 102   | 148.4 | 1.2 |
| UAK02  | ALV-3887-1549-004-004* | Muir | 2,372                | 3,470                      | 0.002                      | 9.01                                     | 0.04   | 0.539            | 0.006             | 143.3                                       | 1.1 | 0.1586 | 0.0007 | 16,258 | 77  | 16,168 | 116   | 150.0 | 1.1 |
| UA114  | ALV-3887-1549-004-005* | Muir | 2,372                | 3,943                      | 0.003                      | 10.12                                    | 0.04   | 0.918            | 0.006             | 140.2                                       | 1.3 | 0.1569 | 0.0007 | 16,113 | 80  | 15,980 | 152   | 146.6 | 1.3 |
| UAF13  | ALV-3887-1549-004-006* | Muir | 2,372                | 3,812                      | 0.002                      | 9.70                                     | 0.04   | 0.925            | 0.010             | 139.2                                       | 1.1 | 0.1556 | 0.0007 | 15,986 | 77  | 15,853 | 150   | 145.6 | 1.2 |
| UAL19  | ALV-3887-1549-004-006* | Muir | 2,372                | 3,922                      | 0.005                      | 10.07                                    | 0.04   | 1.609            | 0.009             | 136.3                                       | 1.3 | 0.1569 | 0.0007 | 16,181 | 81  | 15,947 | 242   | 142.6 | 1.4 |
| UAF11  | ALV-3887-1549-004-007* | Muir | 2,372                | 4,039                      | 0.002                      | 8.36                                     | 0.04   | 0.584            | 0.008             | 139.6                                       | 1.1 | 0.1265 | 0.0006 | 12,822 | 61  | 12,744 | 96    | 144.7 | 1.1 |
| UAF12  | ALV-3887-1549-004-008  | Muir | 2,372                | 4,282                      | 0.002                      | 10.55                                    | 0.05   | 0.592            | 0.009             | 148.3                                       | 1.0 | 0.1506 | 0.0007 | 15,303 | 73  | 15,227 | 103   | 154.8 | 1.1 |
| UA117  | ALV-3887-1549-004-009* | Muir | 2,372                | 3,360                      | 0.002                      | 6.96                                     | 0.03   | 0.159            | 0.007             | 143.3                                       | 1.1 | 0.1266 | 0.0006 | 12,780 | 62  | 12,752 | 67    | 148.5 | 1.2 |
| UAF02  | ALV-3887-1549-004-012* | Muir | 2,372                | 3,286                      | 0.002                      | 6.76                                     | 0.03   | 0.561            | 0.012             | 142.5                                       | 1.1 | 0.1258 | 0.0006 | 12,707 | 61  | 12,616 | 107   | 147.7 | 1.1 |
| UAA5   | ALV-3887-1549-004-014* | Muir | 2,372                | 3,651                      | 0.007                      | 8.99                                     | 0.04   | 0.524            | 0.002             | 144.6                                       | 3.0 | 0.1505 | 0.0007 | 15,348 | 90  | 15,269 | 118   | 151.0 | 3.1 |
| UAL09  | ALV-3887-1549-004-014* | Muir | 2,372                | 3,644                      | 0.002                      | 8.99                                     | 0.04   | 0.327            | 0.007             | 147.3                                       | 1.1 | 0.1508 | 0.0007 | 15,341 | 74  | 15,289 | 89    | 153.8 | 1.1 |
| UAA3   | ALV-3887-1652-005-006* | Muir | 2,265                | 3,637                      | 0.007                      | 9.82                                     | 0.04   | 6.892            | 0.030             | 143.0                                       | 3.0 | 0.1649 | 0.0008 | 16,960 | 101 | 15,934 | 969   | 149.6 | 3.2 |
| UAL12  | ALV-3887-1652-005-006* | Muir | 2,265                | 3,480                      | 0.001                      | 7.16                                     | 0.03   | 0.384            | 0.005             | 142.4                                       | 1.1 | 0.1258 | 0.0005 | 12,705 | 59  | 12,643 | 84    | 147.6 | 1.1 |
| UAF10  | ALV-3887-1652-005-013* | Muir | 2,265                | 3,882                      | 0.002                      | 9.94                                     | 0.04   | 0.719            | 0.008             | 141.4                                       | 1.1 | 0.1564 | 0.0007 | 16,042 | 77  | 15,939 | 125   | 147.9 | 1.2 |
| UAF14  | ALV-3887-1652-005-018* | Muir | 2,265                | 4,071                      | 0.003                      | 0.34                                     | 0.00   | 0.622            | 0.014             | 148.9                                       | 1.2 | 0.0051 | 0.0000 | 489    | 4   | 418    | 61    | 149.1 | 1.2 |
| UAM15  | ALV-3889-1311-001-001* | Muir | 1,719                | 3,977                      | 0.002                      | 11.34                                    | 0.05   | 1.575            | 0.008             | 132.5                                       | 1.1 | 0.1742 | 0.0008 | 18,181 | 89  | 17,950 | 242   | 139.4 | 1.2 |
| UAJ12  | ALV-3889-1311-001-002* | Muir | 1,719                | 4,253                      | 0.002                      | 17.20                                    | 0.07   | 2.689            | 0.021             | 137.2                                       | 1.1 | 0.2471 | 0.0011 | 26,622 | 133 | 26,228 | 407   | 147.8 | 1.2 |
| UAM09  | ALV-3889-1311-001-003  | Muir | 1,719                | 3,332                      | 0.002                      | 12.44                                    | 0.05   | 4.711            | 0.021             | 139.3                                       | 1.1 | 0.2282 | 0.0010 | 24,293 | 122 | 23,438 | 832   | 148.9 | 1.3 |
| UA118  | ALV-3889-1311-001-004  | Muir | 1,719                | 3,193                      | 0.002                      | 8.74                                     | 0.04   | 1.231            | 0.013             | 150.3                                       | 1.1 | 0.1673 | 0.0007 | 17,103 | 82  | 16,884 | 229   | 157.6 | 1.1 |
| UAM12  | ALV-3889-1311-001-005* | Muir | 1,719                | 3,257                      | 0.002                      | 12.88                                    | 0.06   | 3.702            | 0.017             | 135.0                                       | 1.1 | 0.2417 | 0.0010 | 26,020 | 131 | 25,317 | 693   | 145.0 | 1.3 |
| UAA4   | ALV-3889-1311-001-006* | Muir | 1,719                | 3,262                      | 0.007                      | 14.23                                    | 0.06   | 3.177            | 0.014             | 134.0                                       | 3.0 | 0.2665 | 0.0013 | 29,097 | 183 | 28,501 | 607   | 145.3 | 3.3 |

Table 1. Continued.

| Lab ID | Database ID            | Smt. | Depth (m) | 238U (ppm) | 230Th (ppt) | 232Th (ppb) | $\delta^{234}\text{U}_{\text{perm}}\%$ | $(^{230}\text{Th}/^{238}\text{U})$ activity | Raw age (yrs) | Corr age (yrs) | $\delta^{234}\text{U}_{\text{initial}}\%$ |        |        |         |       |         |        |       |     |
|--------|------------------------|------|-----------|------------|-------------|-------------|--|---|---------------|----------------|---|--------|--------|---------|-------|---------|--------|-------|-----|
| UAL13  | ALV-3889-1311-001-006* | Muir | 1,719     | 3.316      | 0.002       | 14.49       | 0.06                                   | 1.011                                       | 0.019         | 135.4          | 1.2                                       | 0.2671 | 0.0012 | 29,121  | 150   | 28,923  | 243    | 146.9 | 1.3 |
| UAL15  | ALV-3889-1311-001-007  | Muir | 1,719     | 3.530      | 0.002       | 9.23        | 0.04                                   | 0.709                                       | 0.010         | 147.9          | 1.1                                       | 0.1598 | 0.0007 | 16,319  | 78    | 16,204  | 136    | 154.8 | 1.1 |
| UAMI0  | ALV-3889-1311-001-008* | Muir | 1,719     | 3.852      | 0.002       | 18.06       | 0.08                                   | 1.649                                       | 0.009         | 139.6          | 1.1                                       | 0.2866 | 0.0012 | 31,434  | 161   | 31,153  | 316    | 152.4 | 1.2 |
| UAMI1  | ALV-3889-1311-001-008* | Muir | 1,719     | 3.711      | 0.002       | 16.78       | 0.07                                   | 9.407                                       | 0.041         | 135.5          | 1.1                                       | 0.2763 | 0.0012 | 30,275  | 155   | 28,660  | 1,540  | 146.9 | 1.3 |
| UAL20  | ALV-3889-1326-002-B7*  | Muir | 1,723     | 3.048      | 0.002       | 47.76       | 0.21                                   | 2.142                                       | 0.011         | 82.1           | 1.2                                       | 0.9575 | 0.0042 | 221,140 | 3,172 | 218,494 | 4,005  | 152.3 | 2.7 |
| UAA2   | ALV-3889-1353-003-001* | Muir | 1,714     | 3.442      | 0.007       | 11.58       | 0.05                                   | 21.778                                      | 0.095         | 145.2          | 3.0                                       | 0.2056 | 0.0010 | 21,518  | 134   | 18,006  | 2,975  | 152.8 | 3.5 |
| UAL08  | ALV-3889-1353-003-001* | Muir | 1,714     | 3.350      | 0.002       | 9.46        | 0.04                                   | 5.420                                       | 0.026         | 146.0          | 1.1                                       | 0.1725 | 0.0008 | 17,752  | 87    | 16,835  | 874    | 153.1 | 1.2 |
| UAA8   | ALV-3889-1526-006-001  | Muir | 1,620     | 3.890      | 0.008       | 55.53       | 0.24                                   | 26.943                                      | 0.115         | 102.2          | 3.0                                       | 0.8723 | 0.0042 | 163,812 | 2,140 | 150,328 | 13,015 | 156.3 | 7.6 |
| UAE08  | ALV-3889-1526-006-001  | Muir | 1,620     | 4.022      | 0.002       | 56.80       | 0.24                                   | 3.052                                       | 0.013         | 97.9           | 1.1                                       | 0.8629 | 0.0037 | 161,549 | 1,619 | 159,899 | 2,249  | 153.8 | 1.9 |
| UAE03  | ALV-3889-1526-006-B2   | Muir | 1,620     | 4.936      | 0.003       | 59.92       | 0.26                                   | 4.284                                       | 0.018         | 120.5          | 5.0                                       | 0.7419 | 0.0032 | 115,159 | 1,340 | 113,946 | 1,754  | 166.2 | 7.0 |
| UAF01  | ALV-3890-1643-005-009  | Muir | 1,487     | 3.318      | 0.005       | 16.75       | 0.08                                   | 2.132                                       | 0.041         | 143.3          | 1.2                                       | 0.3085 | 0.0015 | 34,105  | 197   | 33,694  | 445    | 157.6 | 1.4 |

Table 2. Summary of U-series dated scleractinian corals. In all, 159 measurements were made on 127 coral individuals yielding 99 separate reliable ages. All samples in this table are *Desmophyllum dianthus* except two *Caryophyllia* and one *Solenosmilia* from Gregg and one *Solenosmilia* and two *Enallopsammia* from Manning as marked in Table 1.

| Seamount | Measurements | Individuals | Reliable ages |
|----------|--------------|-------------|---------------|
| Bear     | 3            | 3           | 1             |
| Gregg    | 21           | 15          | 14            |
| Kelvin   | 2            | 2           | 2             |
| Manning  | 65           | 55          | 37            |
| Muir     | 68           | 52          | 45            |
| Total    | 159          | 127         | 99            |

al., 1996). The three oldest population peaks occur close to the times of three Heinrich events, each of which originated in the Hudson Straits (Hemming, 2004). The youngest population peak occurs during the Younger Dryas, which is thought to have a similar water-mass configuration to the Heinrich events (Boyle and Keigwin, 1987).

Changes in ocean circulation appear to have a marked effect on the populations of *D. dianthus* of the New England Seamounts, but determining the cause of the effect is difficult. The fact that no corals were found with LGM ages suggests that the oceanographic configuration was not well suited to coral recruitment and/or growth. Unfortunately, the notch morphology of the sites that were sampled on Muir prevents us from isolating the effect of the presence of deep southern-source water on *D. dianthus* during the LGM. The presence of the shallower (< 2000 m) northern-sourced water does not appear to have been conducive to abundant coral growth.

Rapid encroachments of an intermediate depth (1700–2000 m) southern-source water mass have been recognized in the NW Atlantic at several times during the deglaciation (Adkins et al., 1998; Robinson et al., 2005). The radiocarbon composition from the skeletons of multiple corals recorded the switch from intermediate depth northern to southern-source waters, and vice versa, indicating that *D. dianthus* thrives in conditions in which the ocean is experiencing rapid climate change. Whether these switches brought about beneficial environmental changes (more nutrients, higher current rates?), or allowed coral larvae to reach Muir and Manning Seamounts is unresolved. To best answer this question we would need to make further collections of *D. dianthus* from deep on Muir Seamount, specifically to a second notch feature that extends to greater depths.

**GREGG SEAMOUNT.**—The oldest dated corals from Gregg Seamount, are ~15 ka, and corals are present from throughout the rest of the deglaciation. This age distribution contrasts markedly to they pulsing seen at Muir and Manning, although the sample size is small. The difference between distribution patterns at Gregg and Muir/Manning may be controlled by depth or geographic location. The Gregg samples were all collected from ~1200 m, whereas the shallowest samples from Muir or Manning were at 1400 m. An alternative control may be the relative locations of the three seamounts. Gregg is situated farther northwest than Muir and Manning, close to the position of the modern Gulf Stream. The strong currents of the Gulf Stream may be important in controlling larval dispersal or supply of food to coral populations. The position of the Gulf Stream in the past is not well defined, but shifts in its latitude or velocity may have caused the coral populations in the two locations to be different from one another. To test whether the geographic location or the depth range is the most important control on the age distribution, we would need to collect



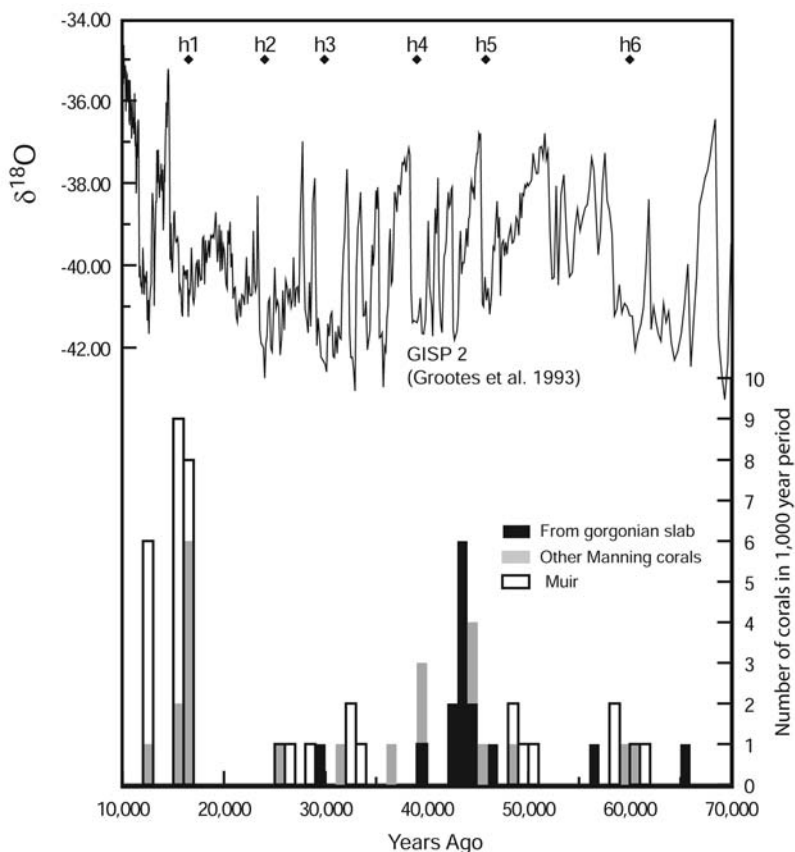


Figure 6. Number of *Desmophyllum dianthus* from Muir (white) and Manning Seamounts. The Manning individuals are divided into those sampled from the build-up pictured in Figure 5 (black) and all other samples (grey). The upper curve is the GISP 2  $\delta^{18}\text{O}$  record from Greenland covering the last glacial period, which lasted from ~70–10 ka. The glacial was characterized by large climate variations shown by the large oscillations in the  $\delta^{18}\text{O}$  signal. In addition, marine records have shown pulses of large quantities of ice-rafted debris during the last deglacial. The last six of these Heinrich events are labeled H1-H6 at ages taken from (Hemming, 2004).

deeper samples from Gregg to compare to the more southerly seamounts. We could also date corals from farther along the seamount chain out towards the Corner Rise Seamounts.

**NW AND NE ATLANTIC AGE DISTRIBUTIONS.**—Fossil corals have been collected from multiple locations including the Southern Ocean and NE Atlantic (Goldstein et al., 2001; Schröder-Ritzrau et al., 2003; Frank et al., 2004; Dorschel et al., 2005). Only from the east Atlantic have sufficient corals been dated to provide a comparison to the age distributions shown in this paper (Schröder-Ritzrau et al., 2003; Frank et al., 2004; Dorschel et al., 2005). Most of the corals dated from the NE Atlantic are colonial species such as *Lophelia pertusa* (Linnaeus, 1758), however Schroeder-Ritzrau et al. (2005) also present ten ages from solitary corals (*D. dianthus* and *Caryophyllia*). The distribution of corals ages from the east Atlantic does not show the strong tendency towards glacial age corals observed in the NW Atlantic. Indeed, more than 60% of the dated corals (colonial and solitary) are modern or Holocene in age. The corals from the east Atlantic range in latitude from 2°N–64°N and from < 80 m to

2306 m water depth, spanning a wide range of geographical and oceanographic settings. When this wide distribution is coupled with the number of samples dated, it becomes impossible to make a statistical comparison between the age distributions in the east and west basins of the North Atlantic.

## CONCLUSIONS

Fossil deep-sea corals provide an ideal archive for recording conditions in the past ocean as their skeletons record a signature of the water mass in which they lived (Smith et al., 1997; Adkins et al., 1998). More simply, their presence or absence over long time periods can help to resolve questions of the major controls on deep-sea coral distributions. Fossil corals collected from the New England Seamounts on three cruises during 2003–2005 show a distinct depth distribution, with *D. dianthus* abundant down to 2500 m and colonial scleractinian corals abundant to depths of 1800 m. The 2500 m maximum depth of a notch feature on Muir seamount may be the most important control on the depth cut-off of *D. dianthus*. U-series analysis ages of *D. dianthus* individuals indicate that the largest number of corals was alive during the last glacial period. Within this time, on Muir and Manning Seamounts, the population density of *D. dianthus* was pulsed, and these pulses coincided with major ocean circulation changes as recorded by other paleoceanographic proxies (Boyle and Keigwin, 1987). *Desmophyllum dianthus* appears to thrive in conditions during which the ocean is experiencing rapid climate change. On Gregg Seamount, the population distribution is more continuous. The difference between Gregg compared to Muir and Manning may be caused either by sample depth (all Gregg samples were shallower than the other Seamounts) or position (Gregg is to the north). We could put tighter constraints on the links between coral distribution and oceanographic change by making collections at greater depths, and exploring different topographic morphologies, from both Gregg and Muir Seamounts.

## ACKNOWLEDGMENTS

We gratefully acknowledge the support of The Comer Foundation for Abrupt Climate Change, The Henry Luce Foundation, The American Chemical Society Petroleum Research Fund, NSF Grant Numbers OCE-0096373 and OCE-0095331, and NOAA OE Grant Number A05OAR4601054. We would also like to thank the crew, the science parties, and the DSV ALVIN and ROV HERCULES pilots on RV ATLANTIS cruise AT7-35 and AT8-1, and the DASS05 expedition to the New England Seamounts.

## LITERATURE CITED

- Adkins, J. F. and D. S. Scheirer. New England Seamounts 2003: AT7-35 Cruise Report. 2003. 95 p.
- \_\_\_\_\_, E. A. Boyle, W. B. Curry, and A. Lutringer. 2003. Stable isotopes in deep-sea corals and a new mechanism for "vital effects". *Geochim. Cosmochim. Acta* 67: 1129–1143.
- \_\_\_\_\_, H. Cheng, E. A. Boyle, E. R. M. Druffel, and R. L. Edwards. 1998. Deep-sea coral evidence for rapid change in ventilation of the deep North Atlantic 15,400 years ago. *Science* 280: 725–728.
- \_\_\_\_\_, G. M. Henderson, S. L. Wang, S. O'Shea, and F. Mokadem. 2004. Growth rates of the deep-sea scleractinia *Desmophyllum cristagalli* and *Enallopsammia rostrata*. *Earth Planet. Sci. Lett.* 227: 481–490.

- Bard, E., R. G. Fairbanks, B. Hamelin, A. Zindler, and H. Chi Trach. 1991. Uranium-234 anomalies in corals older than 150 000 years. *Geochim. Cosmochim. Acta* 55: 2385–2390.
- Bond, Z. A., A. L. Cohen, S. R. Smith, and W. J. Jenkins. 2005. Growth and composition of high-Mg calcite in the skeleton of a Bermudian gorgonian (*Plexaurella dichotoma*): Potential for paleothermometry. *Geochem. Geophys. Geosyst.* Q08010, doi:10.1029/2005GC000911.
- Boyle, E. A. and L. D. Keigwin. 1987. North Atlantic thermohaline circulation during the past 20 000 years linked to high-latitude surface temperature. *Nature* 330: 35–40.
- Broecker, W., S. L. Peacock, S. Walker, R. F. Weiss, V. Fahrenbach, M. Schroeder, U. Mikolajewicz, C. Heinze, R. Key, T. H. Peng, and S. Rubin. 1998. How much deep water is formed in the Southern Ocean? *J. Geophys. Res.* 103: 15,833–15,843
- Broecker, W. S. 1998. Paleocirculation during the last deglaciation: a bipolar seesaw? *Paleoceanography* 13: 119–121.
- \_\_\_\_\_ and T. Takahashi. 1966. Calcium carbonate precipitation on the Bahama Banks. *J. Geophys. Res.* 71: 1575–1602.
- Cheng, H., J. F. Adkins, R. L. Edwards, and E. A. Boyle. 2000. U-Th dating of deep-sea corals. *Geochim. Cosmochim. Acta* 64: 2401–2416.
- \_\_\_\_\_, R. L. Edwards, J. Hoff, C. D. Gallup, D. A. Richards, and Y. Asmeron. 2000. The half-lives of uranium-234 and thorium-230. *Chem. Geol.* 169: 17–33.
- Cohen, A. L., G. D. Layne, S. R. Hart, and P. S. Lobel. 2001. Kinetic control of skeletal Sr/Ca in a symbiotic coral: Implications for the paleotemperature proxy. *Paleoceanography* 16: 20–26.
- Curry, W. B. and D. W. Oppo. 2005. Glacial water mass geometry and the distribution of delta C-13 of Sigma CO2 in the western Atlantic Ocean. *Paleoceanography* 20 PA1017.
- Cutler, K. B., R. L. Edwards, F. W. Taylor, H. Cheng, J. F. Adkins, C. D. Gallup, P. M. Cutler, G. S. Burr, and A. L. Bloom. 2003. Rapid sea-level fall and deep-ocean temperature change since the last interglacial period. *Earth Planet. Sci. Lett.* 206: 253–271.
- Dorschel, B., D. Hebbeln, A. Rüggeberg, W. C. Dullo, and A. Freiwald. 2005. Growth and erosion of a cold-water coral covered carbonate mound in the Northeast Atlantic during the Late Pleistocene and Holocene. *Earth Planet. Sci. Lett.* 233: 33–44.
- Duplessy, J. C., N. J. Shackleton, R. G. Fairbanks, L. Labeyrie, D. W. Oppo, and N. Kallel. 1988. Deep water source variations during the last climatic cycle and their impact on the global deep water circulation. *Paleoceanography* 3: 343–360.
- Edwards, R. L., J. H. Chen, and G. J. Wasserburg. 1986. <sup>238</sup>U-<sup>234</sup>U-<sup>230</sup>Th-<sup>232</sup>Th systematics and the precise measurement of time over the past 500 000 years. *Earth Planet. Sci. Lett.* 81: 175–192.
- Frank, N., M. Paterne, L. Ayliffe, T. van Weering, J. P. Henriot, and D. Blamart. 2004. Eastern North Atlantic deep-sea corals: tracing upper intermediate water Delta C-14 during the Holocene. *Earth Planet. Sci. Lett.* 219: 297–309.
- Freiwald, A. 2002. Reef-forming cold-water corals. Pages 365–385 in G. Wefer, D. Billett, D. Hebbeln, G. Wefer, D. Billett, D. Hebbeln, B. B. Jørgensen, M. Schlüter, and T. C. E. van Weering, eds. *Ocean Margin System*, Springer.
- Gallup, C. D., R. L. Edwards, and R. G. Johnson. 1994. The timing of high sea levels over the past 200 000 years. *Science* 263: 796–800.
- Ganachaud, A. and C. Wunsch. 2000. Improved estimates of global ocean circulation, heat transport and mixing from hydrographic data. *Nature* 408: 453–457.
- Goldstein, S. J., D. W. Lea, S. Chakraborty, M. Kashgarian, and M. T. Murrell. 2001. Uranium-series and radiocarbon geochronology of deep-sea corals: Implications for Southern Ocean ventilation rates and the oceanic carbon cycle. *Earth Planet. Sci. Lett.* 193: 167–182.
- Groote, P. M., M. Stuiver, J. W. C. White, S. Johnsen, and J. Jouzel. 1993. Comparison of oxygen isotope records from the GISP2 and GRIP Greenland ice cores. *Nature* 366: 552–554.
- Heinrich, H. 1988. Origin and consequences of cyclic ice rafting in the northeast Atlantic Ocean during the past 130 000 years. *Quat. Res.* 29: 142–152.

- Hemming, S. R. 2004. Heinrich events: Massive late Pleistocene detritus layers of the North Atlantic and their global climate imprint. *Rev. Geophys.* 42 doi:10.1029/2003RG000128.
- Henderson, G. M. 2002. Seawater (234U/238U) during the last 800 thousand years. *Earth Planet. Sci. Lett.* 199: 97–110.
- Hughen, K. A., J. T. Overpeck, L. C. Peterson, and S. Trumbore. 1996. Rapid climate changes in the tropical Atlantic region during the last deglaciation. *Nature* 380: 51–54.
- Imbrie, J., J. D. Hays, D. G. Martinson, A. McIntyre, A. C. Mix, J. J. Morley, N. G. Pisias, W. L. Prell, and N. J. Shackleton. 1984. The orbital theory of Pleistocene climate: support from a revised chronology of the marine delta O-18 record. Pages 269–305 in A. Berger, J. Imbrie, J. Hays, G. Kukla, and B. Salzman, eds. *Milankovitch and Climate*. Proc. NATO workshop, Reidel; NATO ASI Series C 126.
- Mangini, A., M. Lomitschka, R. Eichstadter, N. Frank, S. Vogler, G. Bonani, I. Hajdas, and J. Patzold. 1998. Coral provides way to age deep water. *Nature* 392: 347–348.
- Marchitto, T. M., Jr., W. B. Curry, and D. W. Oppo. 1998. Millennial-scale changes in North Atlantic circulation since the last glaciation. *Nature* 393: 557–561.
- McManus, J. F., R. Francois, J. M. Gherardi, L. D. Keigwin, and S. Brown-Leger. 2004. Collapse and rapid resumption of Atlantic meridional circulation linked to deglacial climate changes. *Nature* 428: 834–837.
- Meibom, A., M. Stage, J. Wooden, B. R. Constantz, R. B. Dunbar, A. Owen, N. Grumet, C. R. Bacon, and C. P. Chamberlain. 2003. Monthly Strontium/Calcium oscillations in symbiotic coral aragonite: Biological effects limiting the precision of the paleotemperature proxy. *Geophys. Res. Lett.* 30 (7): Article # 1418. doi:10.1029/2002GL01686.
- Mix, A., E. Bard, and R. Schneider. 2001. Environmental processes of the ice age: land, oceans, glaciers (EPILOG). *Quat. Sci. Rev.* 20: 627–658.
- Oppo, D. W. and S. J. Lehman. 1993. Mid-Depth Circulation of the Subpolar North-Atlantic During the Last Glacial Maximum. *Science*: 1148–1152.
- Rahmstorf, S. 1995. Bifurcations of the Atlantic thermohaline circulation in response to changes in the hydrological cycle. *Nature* 378: 145–149.
- Robinson, L. F., N. S. Belshaw, and G. M. Henderson. 2004. U and Th concentrations and isotope ratios in modern carbonates and waters from the Bahamas. *Geochim. Cosmochim. Acta* 68: 1777–1789.
- \_\_\_\_\_, G. M. Henderson, and N. C. Slowey. 2002. U-Th dating of marine isotope stage 7 in Bahamas slope sediments. *Earth Planet. Sci. Lett.* 196: 175–187.
- \_\_\_\_\_, G. M. Henderson, L. Hall, and I. Matthews. 2004. Climatic control of riverine and Seawater uranium-isotope ratios. *Science*. 305: 851–854.
- \_\_\_\_\_, J. F. Adkins, D. P. Fernandez, D. S. Burnett, S.-L. Wang, A. Gagnon, and N. Krakauer. 2006. Primary U-distribution in scleractinian corals and its implications for U-series dating. *Geochem. Geophys. Geosyst.* 7: Q05022, doi:10.1029/2005GC001138.
- \_\_\_\_\_, J. F. Adkins, L. D. Keigwin, J. Southon, D. P. Fernandez, S.-L. Wang, and D. S. Scheirer. 2005. Radiocarbon variability in the Western North Atlantic during the last deglaciation. *Science* 310: 1469–1473.
- Schröder-Kitzrau, A., A. Freiwald, and A. Mangini. 2005. U/Th-dating of deep-water corals from the eastern North Atlantic and the western Mediterranean Sea. Pages 157–172 in A. Freiwald and J. Roberts, eds. *Cold-water corals and ecosystems*, Springer.
- \_\_\_\_\_, A. Mangini, and M. Lomitschka. 2003. Deep-sea corals evidence periodic reduced ventilation in the North Atlantic during the LGM/Holocene transition. *Earth Planet. Sci. Lett.* 216: 399–410.
- Shen, G. T. and E. A. Boyle. 1988. Determination of lead, cadmium and other trace-metals in annually-banded corals. *Chem. Geol.* 67: 47–62.
- Smith, J. E., M. J. Risk, H. P. Schwarcz, and T. A. McConnaughey. 1997. Rapid climate change in the North Atlantic during the Younger Dryas recorded by deep-sea corals. *Nature* 386: 818–820.

Stirling, C. H., T. M. Esat, M. T. McCulloch, and K. Lambeck. 1995. High-precision U-series dating of corals from Western Australia and implications for the timing and duration of the last interglacial. *Earth Planet. Sci. Lett.* 135: 115–130.

ADDRESSES: (L.F.R.) *Department of Marine Chemistry and Geochemistry, Wood Hole Oceanographic Institution, Woods Hole, Massachusetts 02543.* (D.S.S.) *US Geological Survey, 345 Middlefield Rd., MS989, Menlo Park, California 94025.* (J.F.A., D.P.F., A.G.) *CaltechMS 100-23, 1200 E. California Blvd., Pasadena, California 91125.* (R.G.W.) *Department of Biology, Wood Hole Oceanographic Institution, Woods Hole, Massachusetts 02543.* CORRESPONDING AUTHOR: (L.F.R.): *E-mail: <lrobinson@whoi.edu>.*

